Physiological and transcriptomic response of *Medicago truncatula* to colonization with high and low benefit arbuscular mycorrhizal fungi

Kevin R. Cope[1†], Arjun Kafle[1,2,†], Jaya K. Yakha[1], Philip E. Pfeffer[3], Gary D. Strahan[3], Kevin Garcia[2], Senthil Subramanian[1,4], Heike Bücking[1,5*]

[1]South Dakota State University, Biology and Microbiology Department, Brookings, SD 57007 USA

[2]Department of Crop and Soil Sciences, North Carolina State University, Raleigh, NC 27695 USA

[3]USDA, Agricultural Research Service, Eastern Regional Research Center, Wyndmoor, PA, 19038 USA

[4]Department of Agronomy, Horticulture, and Plant Science, South Dakota State University, Brookings, SD, 57007 USA

[5]Division of Plant Science and Technology, University of Missouri, Columbia, MO 65211

[†]These Authors contributed equally to the work.

*Address correspondence to Heike Bücking (heike.buecking@missouri.edu)

Funding. This work was funded by the USDA (2017-67014-26530), the SD Soybean Research and Promotion Council, and the Agricultural Experiment Station at SDSU to HB and SS. KG acknowledges support of the North Carolina Agriculture Research Service

(NCARS), the North Carolina Soybean Producers Association (2019-1656), and the USDA (2020-67013-31800).

ABSTRACT

Arbuscular mycorrhizal (AM) fungi form a root endosymbiosis with many agronomically important crop species and both enhance the ability of their host to obtain nutrients from the soil and increase host tolerance to biotic and abiotic stressors. However, AM fungal species differ in the benefits they provide to their host plants. Here, we examined the putative molecular mechanisms involved in the regulation of the physiological response of *Medicago truncatula* to either *Rhizophagus irregularis or Glomus aggregatum,* a high or a low benefit AM fungus, respectively. Colonization with *R. irregularis* led to higher growth and nutrient uptake benefits than the colonization with *G. aggregatum*. These benefits were linked to an elevated expression in the roots of genes involved in strigolactone biosynthesis (*NSP1*, *NSP2*, *CCD7*, and *MAX1a*), mycorrhiza-induced phosphate (*PT8*), ammonium (*AMT2;3*), and nitrate (*NPF4.12*) transporters and the putative ammonium transporter *NIP1;5*. *R. irregularis* also stimulated the expression of photosynthesis-related genes in the shoot and the upregulation of the sugar transporters *SWEET1.2, SWEET3.3* and *SWEET 12* and the lipid biosynthesis gene *RAM2* in the roots. In contrast, *G. aggregatum* induced the expression of biotic stress defense response genes in the shoots and several genes associated with abiotic stress in the roots. This suggests that either the host perceives colonization by *G. aggregatum* as a pathogen attack or that *G. aggregatum* can prime host defense responses. Our findings

reveal novel insights into the molecular mechanisms that control the host plant response to colonization with high- and low-benefit arbuscular mycorrhizal fungal symbionts.

KEYWORDS

Medicago truncatula, arbuscular mycorrhizal fungi, symbiosis, nutrient exchange, phosphorus, nitrogen, carbon, transporters, and SWEET

INTRODUCTION

Nitrogen (N) and phosphorus (P) are the main nutrients that limit plant growth in natural and agricultural ecosystems (LeBauer and Treseder 2008; Vitousek et al. 2010). Conventional management practices typically address both N and P limitations through the application of chemical fertilizers, but fertilizer production, transportation, and application are both economically and environmentally expensive (Havlin et al. 2014). Implementing more sustainable methods to mitigate nutrient deficiencies in crops is essential to prevent continued environmental degradation and to still meet the nutritional demands of a growing human population.

To overcome nutrient limitations, plants have evolved the capacity to form alliances with mutualistic, root-associated microbes (Martin et al. 2017). The most widespread mutualism is the arbuscular mycorrhizal (AM) symbiosis formed by 72% of all known plant species and a relatively small number of fungal species in the Glomeromycotina (Brundrett and Tedersoo 2018; Spatafora et al. 2016). AM fungi provide the host plant with mineral nutrients, such as P and N, and improve the resistance of plants against abiotic and biotic stressors (Bücking and Kafle 2015; Kafle et al. 2019). Under P

68 deficiency, plants increase the production of strigolactones, a class of phytohormones
69 that also serve as signaling molecules perceived by AM fungi (Yoneyama et al. 2007).
70 Strigolactones are exuded into the rhizosphere through the ATP-binding cassette
71 transporter PDR1 (Kretzschmar et al. 2012). AM fungal perception of strigolactones
72 triggers spore germination, hyphal branching, and the production of short-chain chitin
73 oligomers (Besserer et al. 2008; Genre et al. 2013). These, along with lipo-
74 chitooligosaccharides (Maillet et al. 2011; Rush et al. 2020), comprise the so-called "Myc
75 factors" that prime the host plant for colonization by activating the "common symbiosis
76 signaling pathway" (CSSP; reviewed in MacLean et al., 2017).

77 The key steps of the CSSP include: 1) the perception of Myc factors at the plasma
78 membrane of root epidermal cells by lysine-motif receptor-like kinases (*e.g.*, NFP and
79 LYK3; Feng et al., 2019); 2) the activation of the secondary messenger mevalonate that
80 likely activates multiple nuclear membrane-localized calcium channels (CASTOR,
81 DMI1/POLLUX, and CNGC15); 3) oscillations in calcium ion concentration in the
82 nucleoplasm that activate a calcium- and calmodulin-dependent protein kinase
83 (DMI3/CCaMK; Lévy et al., 2004; Singh and Parniske, 2012); 4) phosphorylation of IPD3
84 which, in concert with DELLA, induces the expression of RAM1; and 5) activation of
85 several other transcription factors required for the development and regulation of the AM
86 symbiosis (Pimprikar et al., 2016; Pimprikar and Gutjahr, 2018). Following root
87 penetration, AM hyphae proliferate both intra- and intercellularly and form highly branched
88 nutrient exchange structures called arbuscules in cortical cells (Park et al. 2015).
89 Surrounding the arbuscule is a plant-derived periarbuscular membrane (PAM) that is
90 enriched in AM-induced transporters that facilitate reciprocal nutrient exchange between

91 the fungus and the plant (Garcia et al. 2016). In *Medicago truncatula*, three AMT2 family
92 ammonium transporters (AMT2;3, AMT2;4, and AMT2;5; Breuillin-Sessoms et al., 2015)
93 and the phosphate transporters *PT4* (Javot et al. 2007) and *PT8* (Breuillin-Sessoms et al.
94 2015) are involved in the uptake of N and P from the periarbuscular space between the
95 fungal plasma membrane and the PAM. In exchange, host plants transfer about 20% of
96 their photosynthetically derived carbon to their fungal partners, and these high carbon
97 costs force host plants to strongly regulate the carbon flux to their fungal symbionts
98 (Wright et al. 1998). The host plant releases lipids and sugars into the mycorrhizal
99 interface likely via the putative lipid transporters *STR* and *STR2* (Zhang et al., 2010; Roth
100 and Paszkowski, 2017) and the bidirectional sugar transporter *SWEET1.2* (formerly
101 SWEET1b, An et al., 2019; Doidy et al., 2019).

102 AM fungi differ in the benefits that they provide for their host plant. The cooperative
103 AM fungus *Rhizophagus irregularis* 09 (Ri09) transfers more N and P to its host plant and
104 contributes to higher mycorrhizal growth responses than the less-cooperative fungus
105 *Glomus aggregatum* 165 (Ga165; Fellbaum et al., 2014). Symbiosis with Ga165 is also
106 more costly for the host plant (measured as carbon costs per P transferred) than with
107 Ri09, and *M. truncatula* preferentially allocates more carbon to Ri09 than to Ga165 (Kiers
108 et al. 2011). Collectively, these studies suggest that carbon to nutrient exchange
109 processes are driven by biological market dynamics, but the molecular mechanisms that
110 regulate these processes are largely unknown. We hypothesized that the host plant
111 regulates the expression of key genes in response to the colonization of AM fungi that
112 differ in the nutrient benefits that they provide for the host. To test this hypothesis, we
113 examined the physiological and transcriptomic responses of the host plant *M. trancatula*

114 to colonization by either high- (Ri09) or low-benefit (Ga165) AM fungal partners under N
115 and P limitation.
116
117 **RESULTS**
118 **Colonization by *Rhizophagus irregularis* 09 leads to greater plant biomass and**
119 **phosphorus and nitrogen uptake than *Glomus aggregatum* 165**
120 We used a dual-compartment pot system to compare the overall benefit that Ga165 and
121 Ri09 provided to *M. truncatula* (**Supplemental Fig. S1**). The percent root length
122 colonization by intraradical hyphae and arbuscules was comparable in roots colonized by
123 either fungus; however, the percent of roots containing vesicles was significantly higher
124 in Ga165-colonized roots (**Fig. 1A**). Arbuscular width was comparable for both species of
125 AM fungi (**Fig. 1B-D**). Compared to non-mycorrhizal (NM) plants, Ri09 colonization
126 resulted in greater shoot and root biomass, whereas Ga165 provided no growth benefits
127 (**Fig. 2A-B**). Both fungi led to increased P content (**Fig. 2C-D**) and concentration
128 (**Supplemental Fig. S2**) in the shoots and roots of their host, but Ri09 transferred more
129 P than Ga165. Nitrogen-15 (^{15}N) enrichment levels in the roots and shoots of NM plants
130 did not exceed natural abundance levels (**Fig. 2E-F**), which confirms that there was no
131 mass flow of ^{15}N from the HC into the RC. Both fungi transferred ^{15}N from the HC to their
132 host, but Ga165 only increased root ^{15}N enrichment, whereas Ri09 increased both root
133 and shoot ^{15}N enrichment. Overall, these data indicate that although Ga165 and Ri09
134 showed similar levels of root colonization, only Ri09 colonization led to increased growth,
135 most likely by providing the host plant with greater access to both P and N.
136

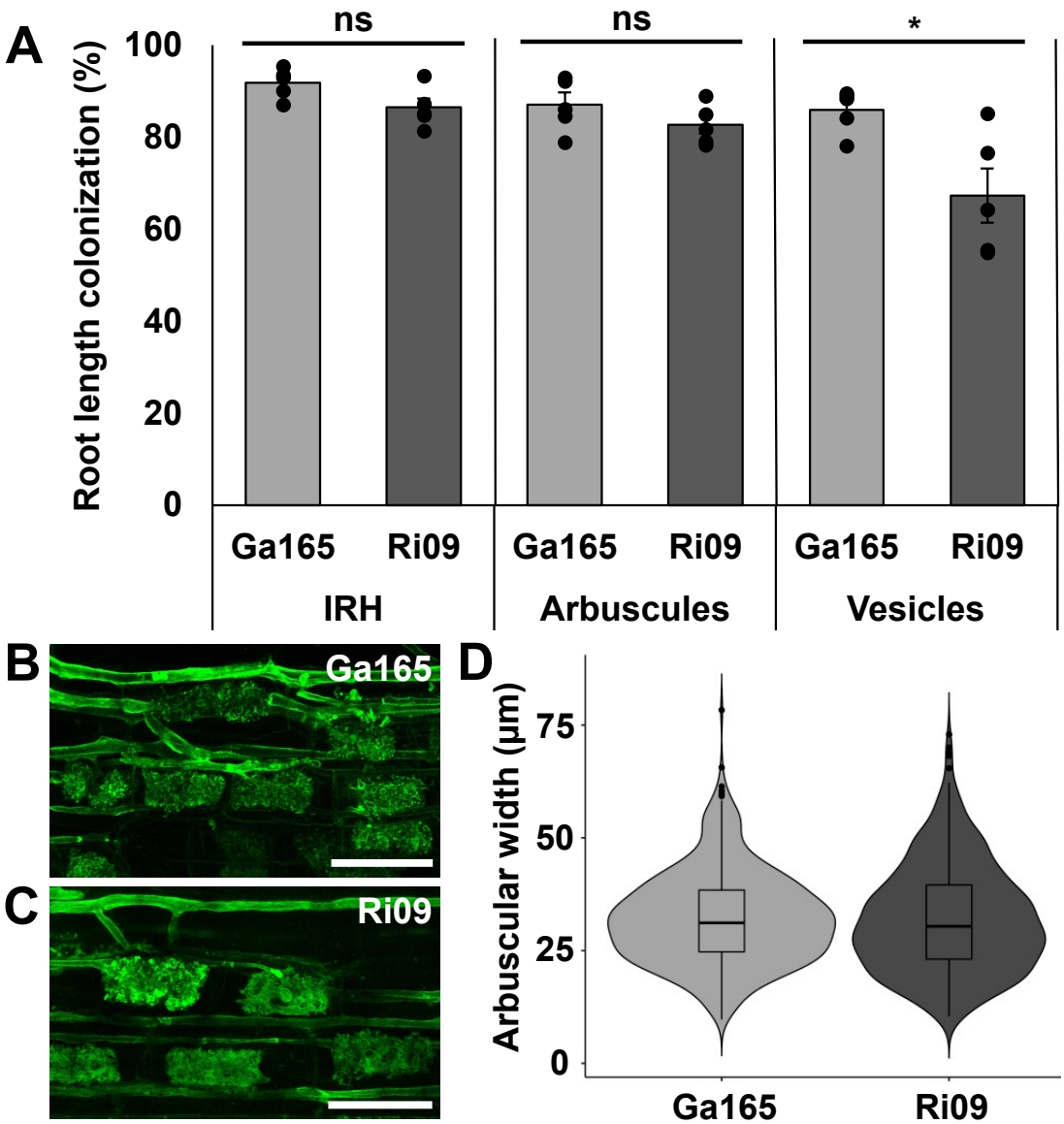

Figure 1. Arbuscular mycorrhizal colonization of *Medicago truncatula* roots and arbuscule size. **A,** percent root length colonization of roots inoculated with *Glomus aggregatum* 165 (Ga165; grey) or *Rhizophagus irregularis* 09 (Ri09; dark grey), measured for intraradical hyphae (IRH), arbuscules, and vesicles. Data points represent individual values for biological replicates (n = 5) and bars represent the mean ± SEM. **B-C**, representative confocal microscope images of Ga165 (**B**) and Ri09 (**C**) arbuscules stained with wheat germ agglutinin conjugated to Alexa Fluor 488. Scale bars = 50 µm. **D**, violin plot of arbuscule widths measured in roots colonized by Ga165 (grey) or Ri09 (dark grey) overlayed with box and whisker plots. In total, 488 and 508 arbuscules were measured in Ga165 and Ri09-colonized roots, respectively. All data were analyzed using a Welch's two-sample t-test and statistically significant differences ($p \leq 0.05$) are indicated with an asterisk.

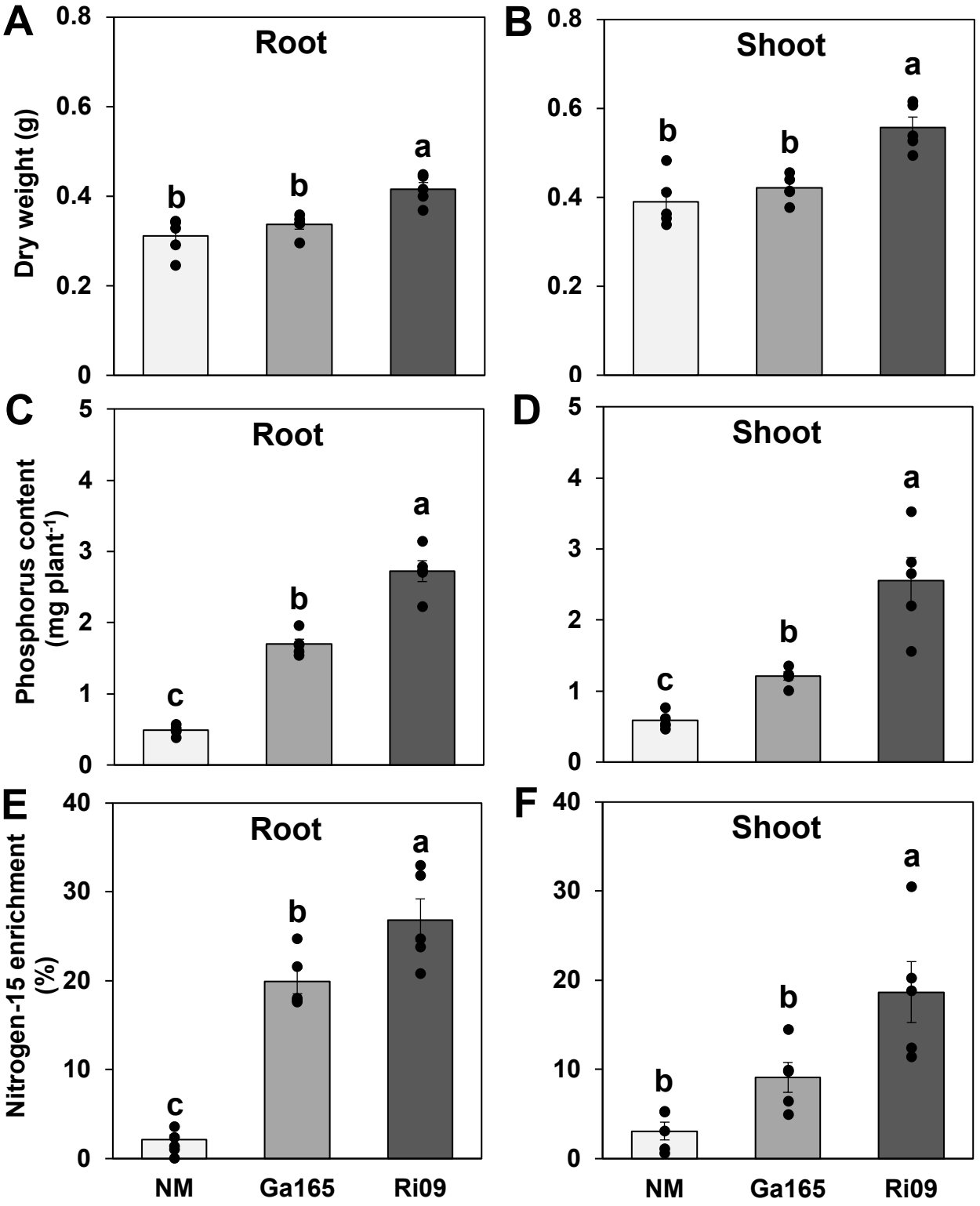

Figure 2. Biomass and nutrient content of *Medicago truncatula* plants colonized by different arbuscular mycorrhizal fungi. Shown are dry weight (**A**,**B**), phosphorus content (**C**,**D**), and % nitrogen-15 enrichment (**E**,**F**) of roots (left) and shoots (right). The plants were inoculated with either *Glomus aggregatum* 165 (Ga165) or *Rhizophagus irregularis* 09 (Ri09) and compared to non-mycorrhizal (NM) control plants. Data points represent individual values for biological replicates (n = 5) and bars represent the mean of each treatment ± SEM. Different letters on the bars indicate statistically significant ($p \leq 0.05$) differences based on one-way ANOVA and LSD test. F statistics and p-values are shown in **Supplemental Table S1**.

137 **Colonization by either fungus alters gene expression more dramatically in the roots**
138 **than in the shoots of *Medicago truncatula***

139 To identify potential molecular mechanisms responsible for the observed physiological
140 responses, we used RNA sequencing (RNA-seq) to evaluate gene expression patterns
141 in roots and shoots of mycorrhizal and non-mycorrhizal plants (**Supplemental File 1**).
142 Analysis of the root data revealed distinct, treatment-specific hierarchical clustering
143 among biological replicates (n=3, Ga165 and NM; n=4, Ri09) using a dendrogram,
144 multidimensional scaling, and principal component analyses (**Supplemental Fig. S3**). In
145 contrast, analysis of the shoot data showed no distinct clustering among biological
146 replicates (n=4, Ga165 and NM; n=3, Ri09) within each treatment (**Supplemental Fig.**
147 **S4**), suggesting that particularly in the roots, gene expression is driven by the fungal
148 partner. Consequently, the overall number of significant differentially expressed genes
149 (DEGs) was lower in the shoots than in the roots (**Supplemental Fig. S5**).

150

151 **Both shared and distinct sets of genes are differentially regulated in *Medicago***
152 ***truncatula* by colonization with either fungus**

153 To identify key differences in the response of the host plant to both fungal species, we
154 sorted all DEGs from each treatment and used an arbitrary threshold of $\log_2$(fold-change)
155 > 2 and a q-value < 0.05 (**Fig. 3A**). In the roots, this threshold revealed that 364 genes
156 were upregulated in roots colonized by either fungus, and 197 or 165 genes were
157 upregulated by colonization with only Ga165 or Ri09, respectively (**Fig. 3B**). Ga165 and
158 Ri09 colonization led to the downregulation of 41 shared genes, and 172 and 77 unique
159 genes, respectively. The clustering of DEGs allowed us to identify specific groups of

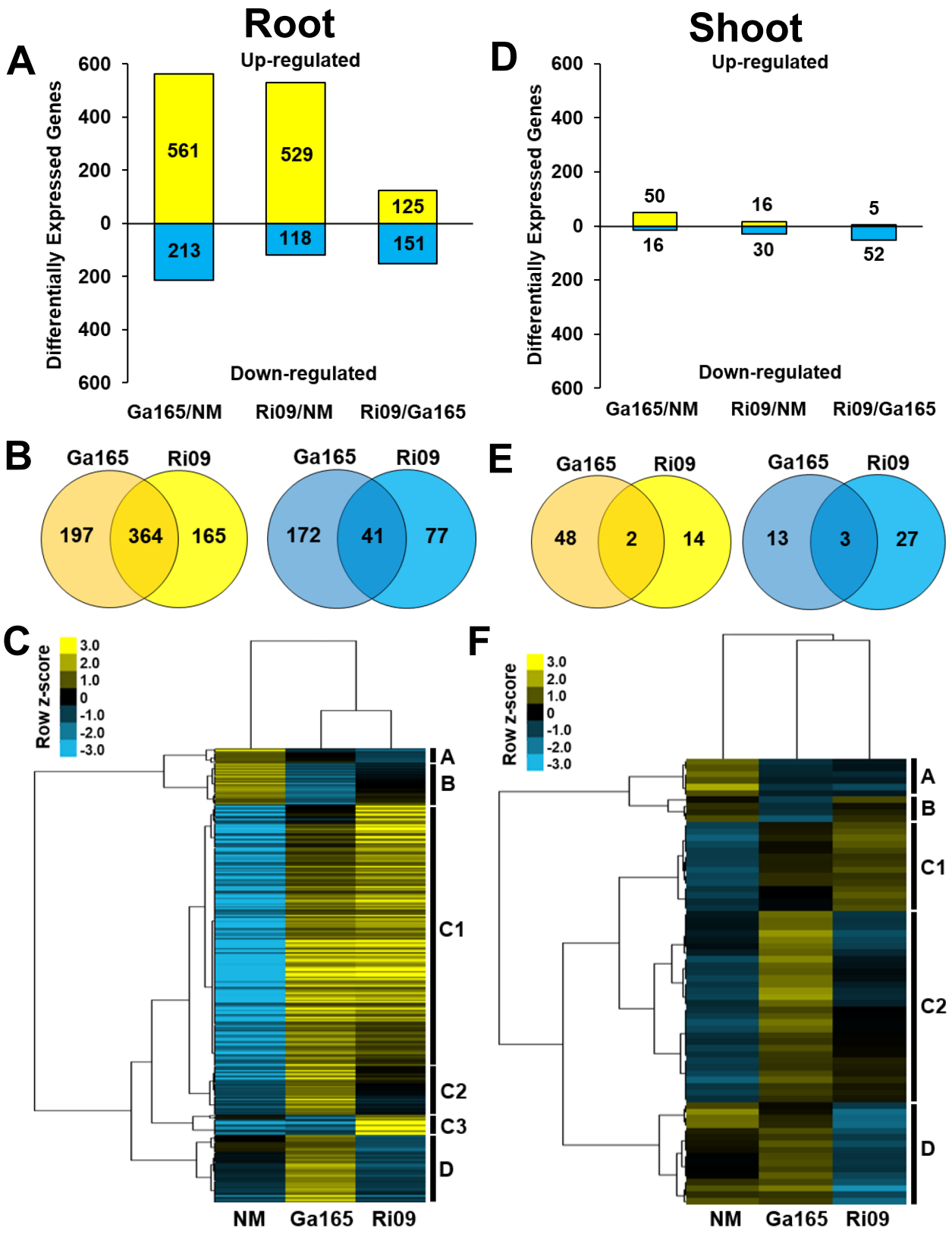

Figure 3. Significantly differentially expressed genes in roots (**A**–**C**) and shoots (**D**–**F**) of *Medicago truncatula* colonized by different AM fungi. **A** and **D**, Number of significantly differentially expressed genes (DEGs; $\log_2$[fold-change] > 2 and a q-value < 0.05) in plants colonized by *Glomus aggregatum* 165 (Ga165) or *Rhizophagus irregularis* 09 (Ri09) compared either to non-mycorrhizal (NM) control plants or to each other. **B** and **E**, Venn diagrams of significantly upregulated (yellow) and downregulated (blue) DEGs unique to Ga165 and Ri09-colonized plants or shared by both. **C** and **F**, Heat maps of fragments per kilobase of transcript per million mapped reads (FPKM) values + 1 for all significant DEGs from each treatment. Gene clusters are assigned based on second-order and sub-clusters based on third- or fourth-order branching. Upregulated genes are shown in yellow and downregulated genes in blue with intensity based on row z-score. All DEGs in each plot for roots and shoots, respectively, are listed in **Supplemental Files 2 and 3**.

160 similarly expressed genes (**Fig. 3C**). Clusters A and B are comprised of genes that were
161 strongly downregulated in mycorrhizal roots, cluster C1 contains genes that were
162 upregulated in mycorrhizal roots, clusters C2 and D include genes primarily upregulated
163 by Ga165 colonization, and cluster C3 contains genes exclusively upregulated by Ri09
164 colonization (**Supplemental File 2)**.

165 Although fewer genes were differentially expressed in the shoots, many were
166 above our applied threshold (**Fig. 3D**). We found that 48 and 14 genes were up, and 13
167 and 27 genes were downregulated in the shoots of Ga165 and Ri09-colonized plants,
168 respectively (**Fig. 3E**). In contrast to the roots, clustering of DEGs based on expression
169 patterns in the shoots (**Fig. 3F)** revealed that only a small number of genes were
170 upregulated (cluster C1) or downregulated (cluster A) in mycorrhizal plants. In addition,
171 some genes were only downregulated by Ga165 (cluster B) or by Ri09 colonization
172 (cluster D), while others were primarily upregulated by Ga165 colonization (cluster C2;
173 **Supplemental File 3**). Collectively, these results demonstrate that compared to shoots,
174 gene expression patterns in roots respond more strongly to colonization with different AM
175 fungi, and that both fungi lead to distinct differences particularly in the root and to a lesser
176 degree also in the shoot transcriptome profiles.

177

178 **Genes critical for the establishment of AM symbiosis are more strongly**
179 **upregulated by *Rhizophagus irregularis* 09 than *Glomus aggregatum* 165**

180 We conducted a targeted analysis of the root RNA-seq data by first evaluating the
181 expression of many genes known to play a role in AM symbiosis (**Supplemental Table**
182 **S2**). Among six core strigolactone biosynthesis or exporter genes (**Fig. 4A**), we observed

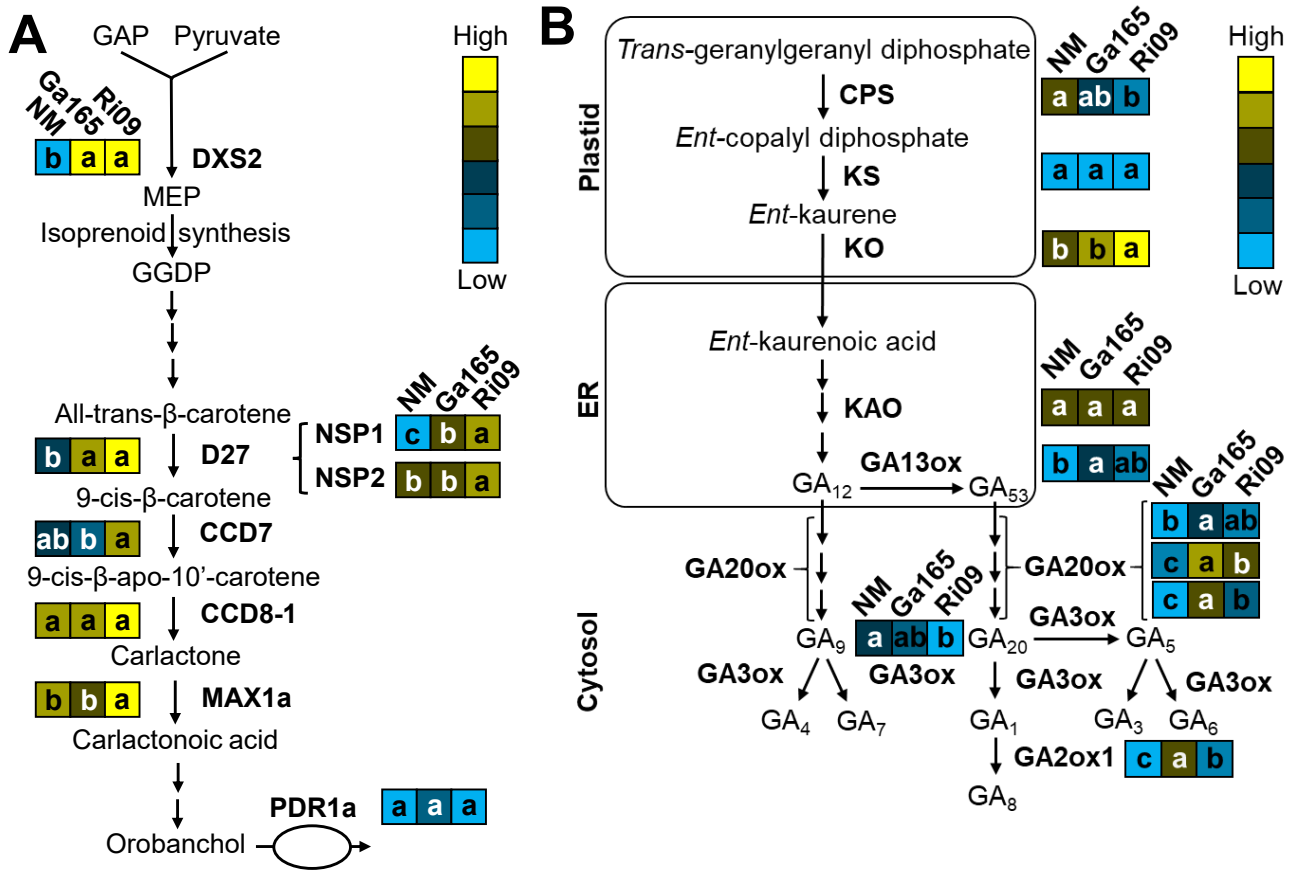

Figure 4. Expression patterns of genes encoding enzymes involved in the strigolactone (**A**) and gibberellic acid (**B**) biosynthesis pathways in the roots of *Medicago truncatula* colonized by arbuscular mycorrhizal fungi. Each diagram portrays the relative expression levels of genes that encode components of the pathways shown as fragments per kilobase of transcript per million mapped reads (FPKM; blue=low, yellow=high) in roots from non-mycorrhizal (NM) plants or plants colonized by either *Glomus aggregatum* 165 (Ga165) or *Rhizophagus irregularis* 09 (Ri09). Letters within boxes indicate significant differences (q-value < 0.05) in FPKM values between treatments and were determined as part of the CuffDiff2 analysis (see **Supplemental Table S2**). Abbreviations: **A**, GAP, glyceraldehyde 3-phosphate; DXS2, 1-deoxyxylulose 5-phosphate synthase2; MEP, 2-methyl-erythritol-4-phosphate; GGDP geranylgeranyl pyrophosphate; D27, Dwarf27; CCD, carotenoid cleavage dioxygenase; and PDR1a, pleiotropic drug resistance 1a. **B**, CPS, *ent*-copalyl diphosphate synthase; KS, *ent*-kaurene synthase; KO, *ent*-kaurene oxidase; KAO, *ent*-kaurenoic acid oxidase; GA13ox, gibberellin 13-oxidase; GA20ox, gibberellin 20-oxidase; GA3ox, gibberellin 3-oxidase; and GA2ox, gibberellin 2-oxidase.

183 that two (*DXS2* and *D27*) were upregulated in AM roots compared to the NM control; one
184 (*MAX1a*) was only upregulated in Ri09-colonized roots, while three (*CCD7*, *CCD8-1* and
185 *PDR1a*) were not affected. Two GRAS transcription factors (*NSP1* and *NSP2*) that
186 regulate strigolactone biosynthesis and other symbiosis genes were also upregulated,
187 particularly in Ri09-colonized roots. The combined increased expression of *NSP1*, *NSP2*,
188 *CCD7*, and *MAX1a* in Ri09-colonized roots compared to Ga165-colonized roots suggests
189 that Ri09 more strongly induces strigolactone biosynthesis than Ga165.

190 Among the CSSP genes, the lipochitooligosaccharide receptor *NFP* was
191 downregulated and *PUB1*, a negative regulator of AM symbiosis (Vernié et al. 2016), was
192 upregulated in roots colonized by either fungus (**Supplemental Table S2**). None of the
193 other 13 analyzed CSSP genes were affected. However, gibberellic acid (GA) is known
194 to play an important role in regulating AM colonization (Floss et al. 2013; Nouri et al.
195 2021), and several genes regulating the biosynthesis and degradation of GA were
196 differentially expressed by mycorrhizal colonization (**Fig. 4B**). In Ri09-colonized roots, the
197 expression of the genes encoding *ent*-copalyl diphosphate synthase (*CPS*) and
198 GA3oxidase (*GA3ox*) were down-regulated compared to NM roots, but the gene encoding
199 *ent*-kaurene oxidase (*KO*) was upregulated. In Ga165-colonized roots, four GA
200 biosynthesis genes (*GA13ox* and three homologs of *GA20ox*) were significantly
201 upregulated compared to NM roots. In Ri09-colonized roots also two of the *GA20ox*
202 homologs were upregulated, but not as strongly as by GA165. Similarly, the GA
203 degradation gene *GA2ox1* was also upregulated in mycorrhizal roots, but more strongly
204 in Ga165-colonized roots (**Supplemental Table S2**).

205 Given the higher expression of more GA biosynthesis genes in Ga165 compared
206 to Ri09-colonized roots, we hypothesize that GA plays a stronger role in regulating the
207 symbiosis with GA165. Therefore, we evaluated the expression of genes downstream of
208 of the CSSP and DELLA1/2, which are proteins that are negatively regulated by GA
209 (Davière and Achard 2013). We evaluated the expression of 21 genes (**Supplemental**
210 **Table S3**), including: seven AM-induced transcription factors that regulate arbuscule
211 development, function, or degradation — *DIP1*, *RAD1*, *RAM1*, *MIG1*/*2*/*3*, and *MYB1*;
212 three cellular remodeling genes — *EXO70I*, *SYP132A*, and *VAPYRIN*; two phosphate
213 transporters (*PT4* and *PT8*); three ammonium transporters (*AMT2;3*, *AMT2;4*, and
214 *AMT2;5*); the putative lipid transporters *STR* and *STR2* and three lipid biosynthesis genes
215 — *RAM2*, *FatM*, and *WRI5a*; and the sugar transporter *SWEET1.2*. Almost all these
216 genes were upregulated by both AM fungal species; however, six were substantially more
217 upregulated by Ri09, including: *RAD1*, *MYB1*, *PT8*, *AMT2;3*, *RAM2*, and *SWEET1.2* (**Fig.**
218 **5A-F**). Together with the physiological results, the increased upregulation of *PT8*,
219 *AMT2;3*, and *SWEET1.2* in Ri09-colonized roots is suggestive of greater nutrient
220 exchange activity across the PAM than in Ga165-colonized roots.
221

222 **Colonization with *Glomus aggregatum* 165 and *Rhizophagus irregularis* 09**
223 **differentially affect the expression of transporters**

224 Gene ontology (GO) enrichment analysis revealed several cellular components,
225 molecular functions, and/or biological processes that were significantly enriched among
226 genes that are only upregulated (**Supplemental Fig. S6**) or downregulated in AM roots
227 (**Supplemental Fig. S7**). Predominant among these were GO terms related to

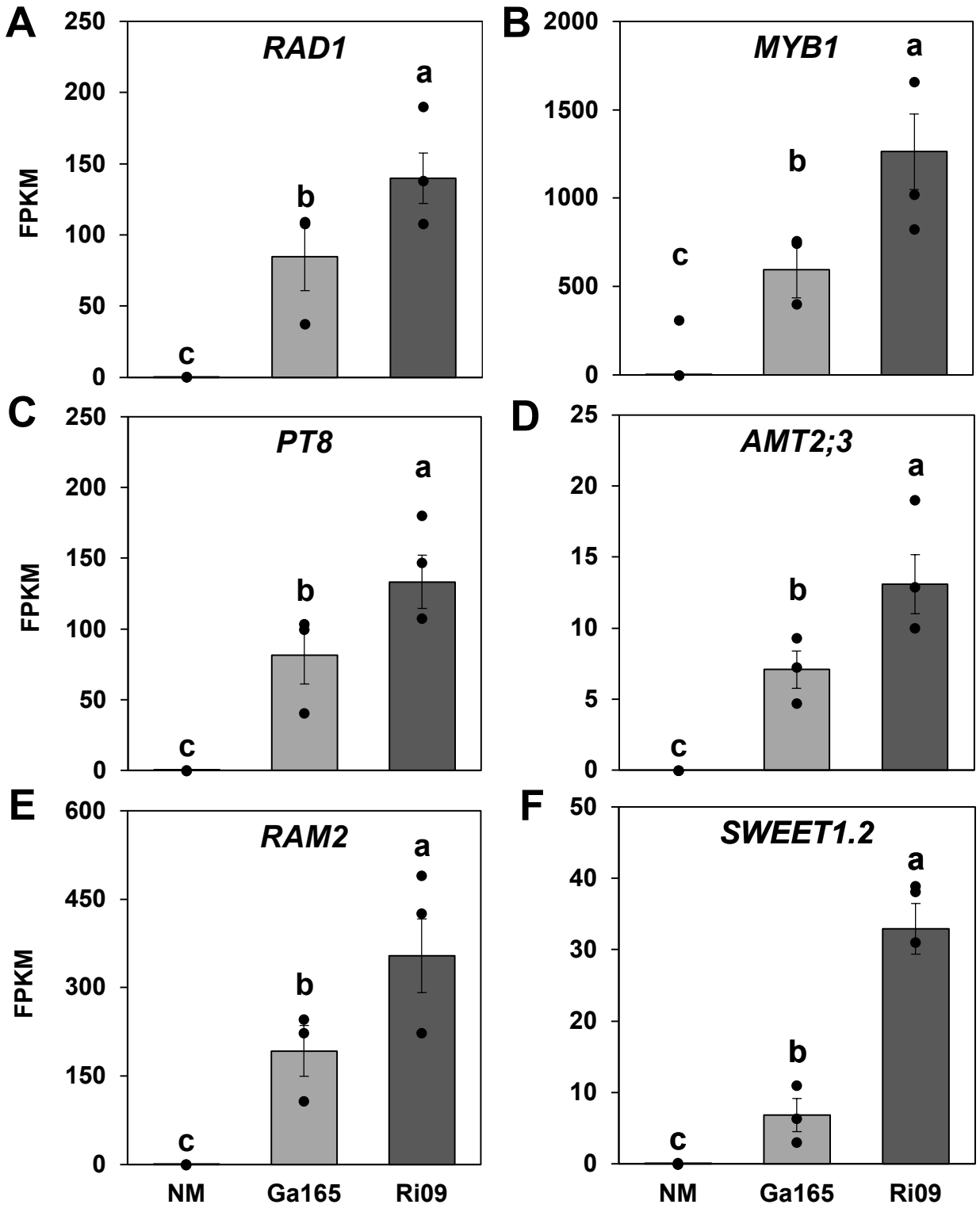

Figure 5. Relative expression of six genes in the roots of *Medicago truncatula* after colonization with different arbuscular mycorrhizal fungi. Expression of **A**, *Required for Arbuscule Development 1* (*RAD1*); **B**, *MYB-like Transcription Factor 1* (*MYB1*); **C**, *Phosphate Transporter 8* (*PT8*); **D**, *Ammonium Transporter 2;3* (*AMT2;3*); **E**, *Reduced Arbuscular Mycorrhization 2* (*RAM2*); and **F**, *Sugars Will Eventually Be Exported Transporter 1.2* (*SWEET1.2*) in the roots of non-mycorrhizal plants (NM, n=3) and plants inoculated with *Glomus aggregatum* 165 (Ga165, n=3) or *Rhizophagus irregularis* 09 (Ri09, n=4). Expression levels are shown as fragments per kilobase of transcript per million mapped reads (FPKM). Data points represent individual values for biological replicates (n = 5) and bars represent the mean of each treatment ± SEM. Significant differences (q-value < 0.05) in FPKM values between treatments were determined as part of the CuffDiff2 analysis and are indicated using different letters (see **Supplemental Table S3**).

228 transmembrane transport. We filtered all gene annotations containing the term “transport”
229 from the *M. truncatula* JCVI 4.0v2 annotation file (Tang et al. 2014) and found 259 genes
230 that were significantly differentially regulated in mycorrhizal roots (**Supplemental File 5**).
231 Based on their function, we further subdivided these genes into two groups: transport of
232 mineral nutrients (72 genes) and secondary metabolites (187 genes). Compared to NM
233 roots, 12 mineral transporters were up- and 17 were down-regulated by both AM fungi
234 (**Fig. 6A**). This suggests that a core set of mineral transporters in AM roots are similarly
235 regulated independent of fungal benefits. However, a unique set of transporters were
236 differentially regulated by each AM fungal species: 14 were up- and 13 were down-
237 regulated in Ga165-colonized roots, while only 7 were up- and 12 were down-regulated
238 in Ri09-colonized roots. From the identified 16 groups of mineral transporters (**Fig. 6B**),
239 we focused on ammonium, nitrate, phosphate, and sulfate transporters with FPKM ≥ 10,
240 due to the key role that AM fungi play in the transport of these nutrients (**Fig. 6C-F**).
241 Among the five differentially regulated ammonium transporters, one belongs to the AMT1
242 ammonium transporter family and four to the AMT2 family. Compared to AM roots,
243 *AMT1;1* and two of the AMT2 family transporters (*AMT2;1* and *AMT2;6*) were highly
244 expressed in NM roots, while *AMT2;3* and *AMT2;5* were specifically induced in
245 mycorrhizal roots. *AMT2;3* was particularly up-regulated in Ri09-colonized roots (**Fig.
246 6C**).

247 We also identified seven differentially regulated nitrate transporters (**Fig. 6D**). Five
248 belong to the nitrate/peptide transporter (NPF) family, and two are putative nitrate
249 transporters. Interestingly, the most highly expressed nitrate transporter (*NPF4.12*) was
250 highly upregulated in AM roots, particularly in Ri09-colonized roots. In contrast, five nitrate

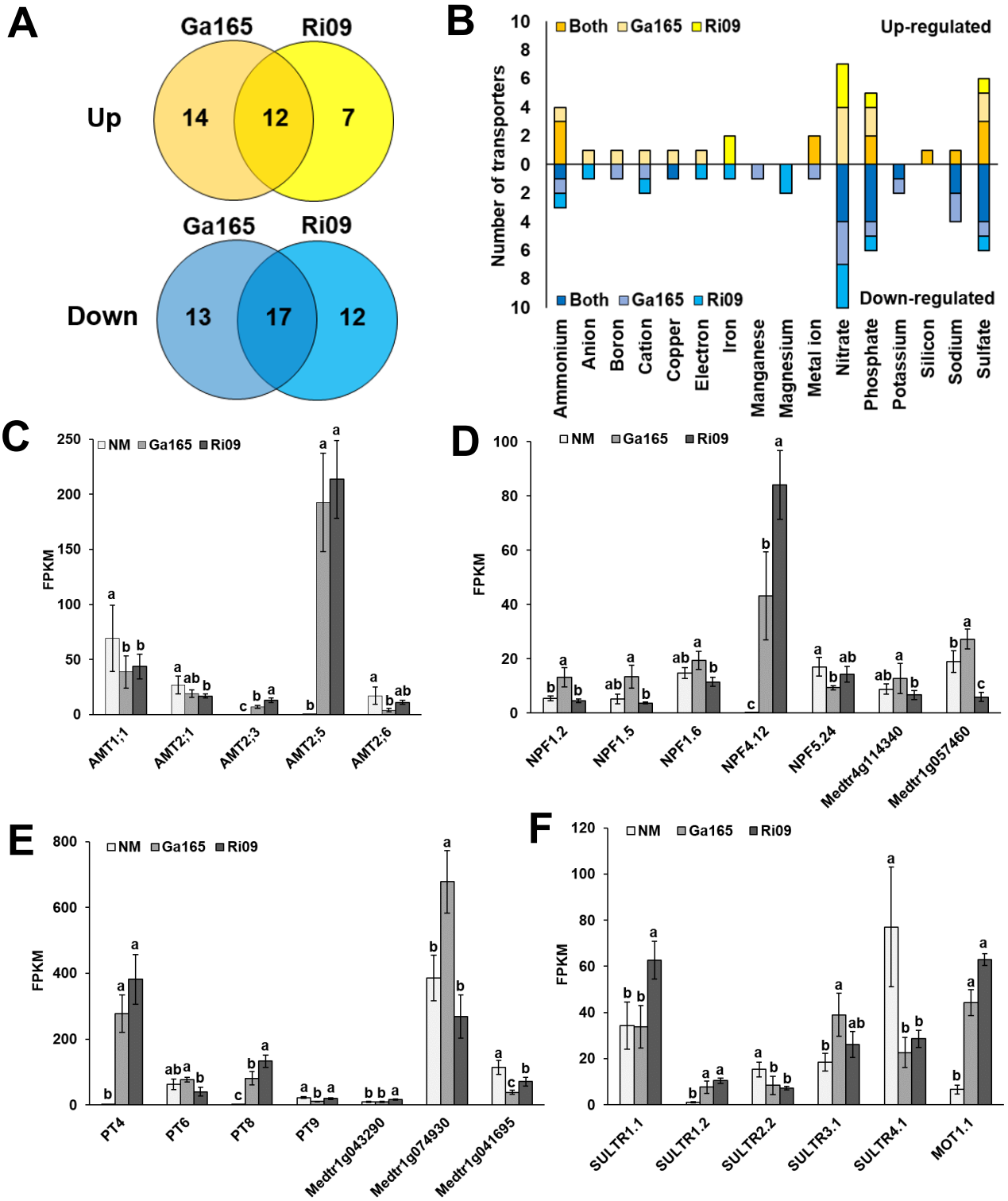

Figure 6. Expression patterns of significantly differentially expressed mineral transporter genes in the roots of *Medicago truncatula* after colonization with different arbuscular mycorrhizal fungi. **A**, Venn diagrams showing the number of mineral transporters that are significantly up- (yellow) or down-regulated (blue) in roots colonized by *Glomus aggregatum* 165 (Ga165) or *Rhizophagus irregularis* 09 (Ri09), or both. **B**, summary of the number of genes from specific gene annotation groups of mineral transporters that are up- or down-regulated in roots colonized by Ga165 or Ri09, or both (see also **Supplemental File 6**). Expression patterns of genes annotated as **C**, ammonium; **D**, nitrate; **E**, phosphate; and **F**, sulfate transporters in the roots of non-mycorrhizal plants (NM; n=3) and plants inoculated with Ga165 (n=3) or Ri09 (n=4). The bars in C–F represent the mean of each treatment ± SEM (data points for biological replicates are displayed in **Supplemental Figure S8**). Expression levels are shown as fragments per kilobase of transcript per million mapped reads (FPKM), only genes with FPKM ≥ 10 are shown, significant differences (q-value < 0.05) in FPKM values between treatments were determined as part of the CuffDiff2 analysis and are indicated using different letters on the bars.

251 transporters were more highly expressed in Ga165-colonized roots than in Ri09-colonized
252 roots (*NPF1.2*, *NPF1.5*, *NPF1.6*, *Medtr4g114340*, and *Medtr1g057460*), and two (*NPF1.2*
253 and *Medtr1g057460*) also differed from control roots. Only the nitrate transporter *NPF5.24*
254 and *Medtr1g057460* showed higher expression in NM roots than in AM-colonized roots.

255 Seven phosphate transporters were differentially regulated (**Fig. 6E**). Four belong
256 to the high-affinity inorganic phosphate transporter family PHT1 (*PT4*, *PT6*, *PT8*, and
257 *PT9*), two were annotated as high-affinity inorganic phosphate transporters
258 (*Medtr1g043290* and *Medtr1g074930*), and one as a phosphate transporter PHO1-like
259 protein. As expected, two of the PHT1 transporter genes, *PT4* and *PT8*, were only
260 expressed in AM roots, and *PT8* expression was higher in Ri09-colonized roots. By
261 contrast, the expression of *Medtr1g074930* was strongly upregulated in Ga165-colonized
262 roots compared to NM and Ri09-colonized roots. The PHO1-like transporter
263 (*Medtr1g041695*) showed higher expression levels in NM than in AM roots.

264 We identified six sulfate transporters that were differentially regulated among the
265 three treatments (**Fig. 6F**). Two were annotated as high affinity sulfate transporter 1
266 (SULTR1) family genes (*SULTR1.1* and *1.2*), three as sulfate/bicarbonate/oxalate
267 exchanger and transporter genes (*SULTR2.2*, *3.1*, and *4.1*), and one as a sulfate
268 transporter-like gene (*MOT1.1*). While the expression levels of *SULTR2.2* and *SULTR4.1*
269 were higher in NM roots than in AM roots, the remaining sulfate transporters were
270 upregulated by colonization with Ri09 (*SULTR1.1*), Ga165 (*SULTR3.1*), or by both fungi
271 (*SULTR1.2* and *MOT1.1*).

272 In total, we identified 20 groups of secondary metabolite transporters in our
273 dataset. Compared to NM control roots, 29 of these transporters were up- and 43 were

274 downregulated in AM roots (**Fig. 7A**). Several secondary metabolite transporters were
275 differentially regulated in Ga165 and Ri09-colonized roots. Among these, most belonged
276 to six gene annotation groups, including ATP-binding cassette (ABC), amino acid, major
277 facilitator superfamily (MFS), major intrinsic protein (MIP), peptide, and Sugars Will
278 Eventually be Exported Transporters (SWEETs) (**Fig. 7B**). Here, we will only discuss
279 those transporters that are known to play a role in AM symbiosis, or that were strongly
280 differentially regulated by mycorrhizal colonization, but have not yet been functionally
281 characterized.

282 Two white-brown-complex ABC transporter family proteins (*STR* and *STR2*; Zhang
283 et al., 2010), three ABC transporter B family proteins (*AMN2*, *AMN3* [Roy, 2015], and
284 *Medtr4g124040*), and one drug resistance transporter-like ABC domain protein
285 (*Medtr1g050525*) were strongly upregulated in AM roots, particularly in Ri09-colonized
286 roots (**Fig. 7C**). The expression levels in Ga165-colonized roots were higher but did not
287 always differ significantly from the NM roots.

288 Two amino acid transporters, *Medtr1g030660* and *Medtr2g101920*, and two
289 peptide transporters, *PTR3* and *OPT15*, were upregulated in mycorrhizal roots (**Fig. 7D**).
290 As expected, *NOPE1,* an N-acetylglucosamine transporter of the major facilitator
291 superfamily (MFS) that is required for AM symbiosis (Nadal et al. 2017), was also highly
292 upregulated in AM roots (**Fig. 7E**). Three major intrinsic protein (MIP) transporters,
293 *NIP1;5*, *NIP1;6*, and *NIP3;1*, which are often classified as aquaporins, were all
294 upregulated in mycorrhizal roots. *NIP1;5* was particularly highly expressed in Ri09-
295 colonized roots, while *NIP1;6*, *NIP3;1* and *NIP6;2* showed higher expression levels in
296 Ga165-colonized roots.

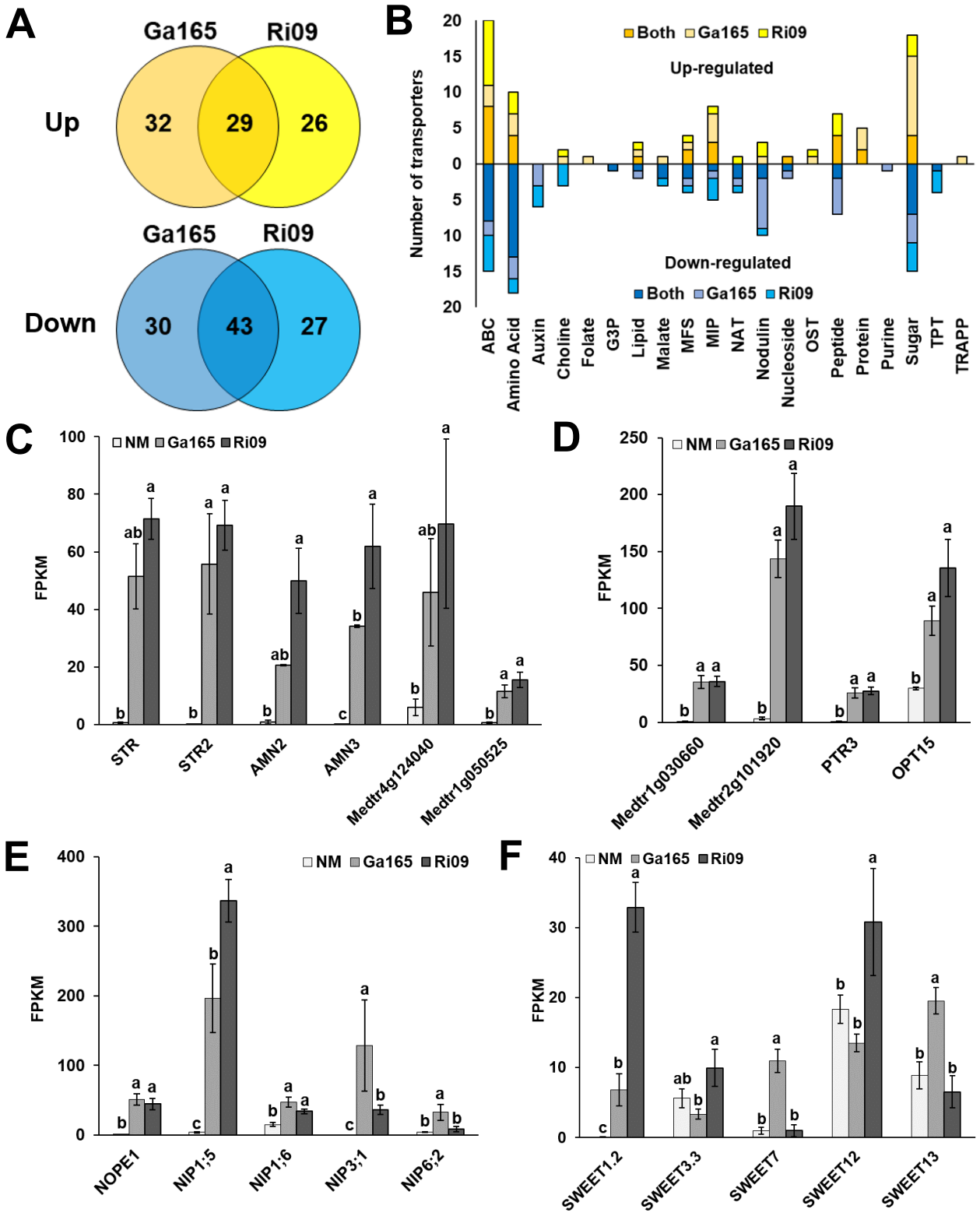

Figure 7. Expression patterns of significantly differentially expressed secondary metabolite transporters in the roots of *Medicago truncatula* after colonization with different AM fungi. **A**, Venn diagrams showing the number of secondary metabolite transporters that are significantly up- (yellow) or down-regulated (blue) in roots colonized by *Glomus aggregatum* 165 (Ga165) or *Rhizophagus irregularis* 09 (Ri09), or both. **B**, summary of the number of genes from specific gene annotation groups of secondary metabolite transports that are up- or down-regulated in roots colonized by Ga165 or Ri09, or both (see **Supplemental File 7**). Expression patterns of genes annotated as **C**, ATP-binding cassette (ABC); **D**, amino acid or peptide; **E**, major facilitator superfamily (MFS) or major intrinsic protein (MIP); and **F**, SWEET transporters in the roots of non-mycorrhizal plants (NM; n = 3) and plants inoculated with Ga165 (n =3) or Ri09 (n = 4). The bars in C-F represent the mean of each treatment ± SEM (data points for biological replicates are displayed in **Supplemental Figure S9**). Expression levels are shown as fragments per kilobase of transcript per million mapped reads (FPKM); only genes with FPKM ≥ 10 are shown; significant differences (q-value < 0.05) in FPKM values between treatments were determined as part of the CuffDiff2 analysis and are indicated using different letters on the bars. Abbreviations in B: G3P, glycerol-3-phosphate; NAT, nucleobase-ascorbate transporter; OST, organic solute transporter; TPT, triose-phosphate transporter; TRAPP, transport protein particle.

297 SWEETs are known to play a crucial role in AM symbiosis (Doidy et al. 2019), and
298 five were differentially expressed in AM roots. *SWEET1.2* was upregulated by
299 colonization with either fungus, but especially with Ri09. *SWEET3.3* and *SWEET12,* were
300 only upregulated in Ri09-colonized roots, whereas *SWEET7* and *SWEET13* were only
301 upregulated in Ga165-colonized roots (**Fig. 7F**). The variation in the expression patterns
302 of these five *SWEET* genes suggests that sugar transport is strongly regulated in
303 response to fungal benefit.
304

305 **Photosynthesis-related genes in the shoots are upregulated in response to**
306 **colonization with *Rhizophagus irregularis* 09**

307 GO enrichment analysis on several gene clusters shown in **Fig. 2F** revealed that cellular
308 components and biological processes associated with photosynthesis were enriched in
309 the shoots of Ri09-colonized plants (**Supplemental Fig. S10A**). The associated genes
310 were annotated as follows: *Medtr1g115410*, photosystem II reaction center family protein
311 (orthologous to PsbP in *Arabidopsis thaliana*); *Medtr2g082580*, oxygen-evolving
312 enhancer protein (orthologous to PsbQ-like protein 2 in *A. thaliana*); *Medtr5g018670*,
313 photosystem II oxygen-evolving enhancer protein; *Medtr1g015290*, ultraviolet-B-
314 repressible protein (orthologous to PsbX in *A. thaliana*); and *Medtr1588s0010*, ATP
315 synthase F1, gamma subunit. The expression levels of *PsbP*, *PsbQ-like protein 2*, *PsbX*,
316 and the ATP synthase gene were significantly higher in the shoots of Ri09-colonized
317 plants than in NM plants (**Fig. 8A**). Out of these genes, only *PsbP* was also significantly
318 upregulated in Ga165-colonized plants. By contrast, *Medtr5g018670* was more highly
319 expressed in the shoots of Ga165-colonized than in NM plants. Overall, these expression

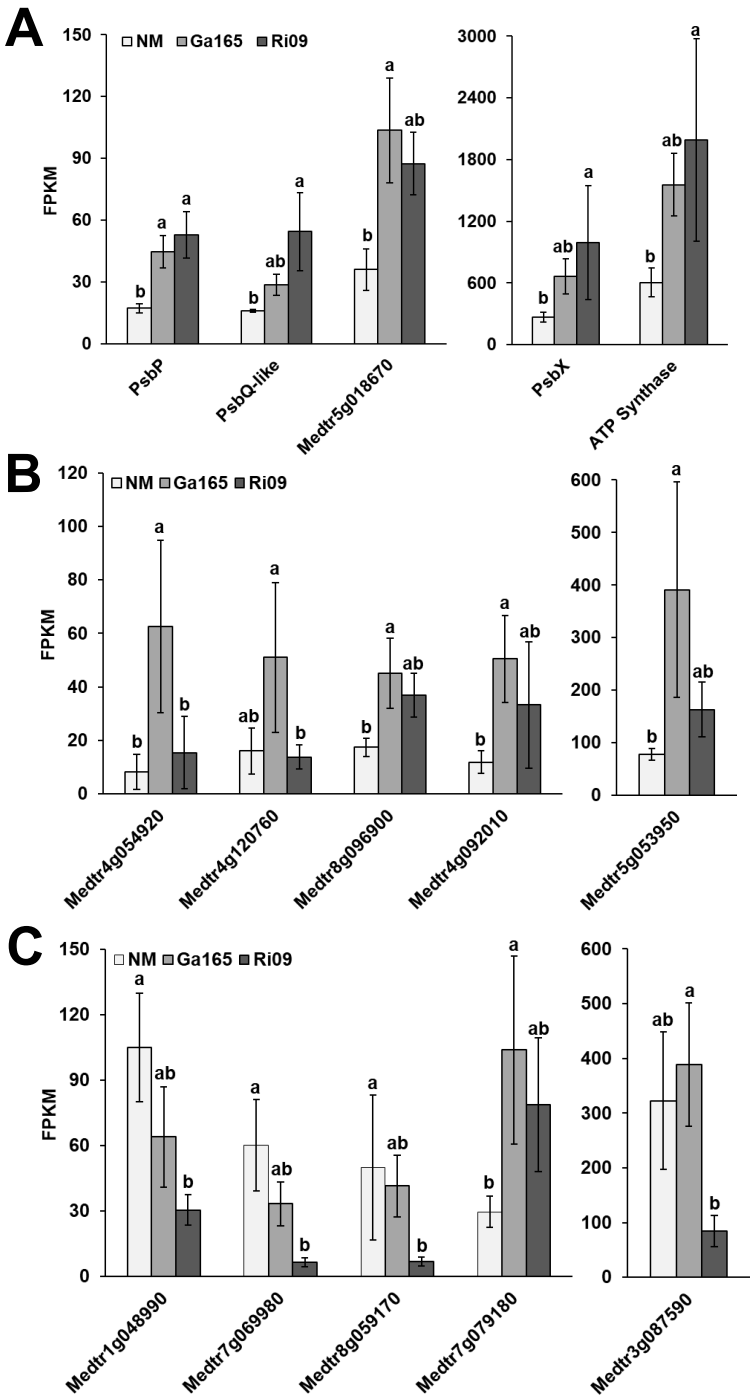

Figure 8. Expression patterns of significantly differentially expressed genes in the shoots of *Medicago truncatula* colonized by different AM fungi. Expression levels of genes involved in **A**, photosynthesis; **B**, response to biotic stress; and **C**, response to abiotic stress in non-mycorrhizal plants (NM; n=4) or plants colonized by *Glomus aggregatum* 165 (Ga165, n=4) or *Rhizophagus irregularis* 09 (Ri09, n=3). Bars represent the mean of each treatment ± SEM (data points for biological replicates are displayed in **Supplemental Figure S11**). Expression levels are shown as fragments per kilobase of transcript per million mapped reads (FPKM), and significant differences (q-value < 0.05) in FPKM values between treatments were determined as part of the CuffDiff2 analysis and are indicated using different letters above the bars (see also **Supplemental Table S4**).

320 patterns imply that photosynthesis was more strongly induced in the shoots of Ri09-
321 colonized plants, which could partially explain the increased biomass of Ri09-colonized
322 plants.
323
324 **Biotic and abiotic stress-related genes are differentially regulated in the shoots of**
325 ***Glomus aggregatum* and *Rhizophagus irregularis* colonized plants**
326 Many of the GO terms that were enriched in the shoots of Ga165-colonized plants
327 encompassed biological processes related to biotic stress (**Supplemental Fig. S10B**).
328 The genes linked to these GO terms were annotated as: *Medtr4g054920*, cytochrome
329 P450 family 94 protein; *Medtr4g120760*, pathogenesis-related protein bet V I family
330 protein; *Medtr8g096900,* pathogenesis-related thaumatin family protein; *Medtr4g092010*,
331 (3S)-linalool/(E)-nerolidol/(E,E)-geranyl linalool synthase; and *Medtr5g053950*, allene
332 oxide cyclase. Enrichment of these GO terms in the shoots of Ga165-colonized plants
333 could indicate that the host plant is responding to Ga165 as it would to a pathogen by
334 upregulating defense responses, or that Ga165 stimulates host plant defenses against
335 pathogens (**Fig. 8B**).
336 In contrast, Ri09 colonization led to the downregulation of genes (**Fig. 3F**, cluster
337 D), associated with biotic and abiotic stress (**Supplemental Fig. S10C**). The genes
338 included in these GO terms were annotated as: *Medtr1g048990*, superoxide dismutase;
339 *Medtr7g069980*, ferritin; *Medtr8g059170*, NAC transcription factor-like protein;
340 *Medtr7g079180*, late embryogenesis abundant protein; and *Medtr3g087590*, myo-inositol
341 1-phosphate synthase. The expression of *Medtr7g079180* was upregulated by Ga165,
342 but the remaining abiotic stress response genes were more highly expressed in NM or

343 Ga165-colonized plants than in Ri09-colonized plants (**Fig. 8C**). Collectively, the
344 expression patterns of these abiotic stress response genes could indicate that Ri09 is
345 more effective at conferring abiotic stress tolerance to *M. truncatula* than Ga165.
346

347 **DISCUSSION**

348 **The growth and nutritional benefits of arbuscular mycorrhizal fungi are linked to**
349 **mycorrhiza-induced transporter expression**

350 When compatible host plants are inoculated with AM fungi, colonization most often leads
351 to increased growth and nutrient uptake, especially in nutrient-deprived conditions
352 (Chandrasekaran 2020). We found that under N and P limitation, Ga165 and Ri09
353 colonized *M. truncatula* equally well (**Fig. 1**), but still, Ri09 promoted greater growth and
354 provided more N and P to the host than Ga165 (**Fig. 2**). This observation is consistent
355 with both the expression patterns that we observed for mycorrhiza-induced N and P
356 transporters and with previous findings where we demonstrated that Ri09 is more
357 cooperative than Ga165 (Kiers et al. 2011; Fellbaum et al. 2014; Wang et al. 2016). For
358 example, the known AM-induced ammonium transporters *AMT2;3* and *AMT2;5* were both
359 upregulated by Ga165 and Ri09 (**Fig. 6C**). Although the expression levels of *AMT2;3* in
360 AM roots were lower than that of *AMT2;5*, *AMT2;3* expression was more strongly
361 upregulated by Ri09 than by Ga165 colonization. Similarly, we observed the same
362 expression pattern for the putative ammonium transporter *NIP1;5* (**Fig. 7E**), which has
363 not been functionally characterized in *M. truncatula* during AM symbiosis, but the soybean
364 ortholog *Nod26* plays a crucial role in ammonium transport in the rhizobia-legume
365 symbiosis (Frare et al. 2018). Interestingly, although the AM fungi were provided with

366 $^{15}NH_4Cl$ as a N source, we also found that the nitrate transporter *NPF4.12* was strongly
367 induced in AM roots, especially in Ri09-colonized roots (**Fig. 6D**). Aloui et al. (2018) found
368 that *NPF4.12* is enriched in the proteome of mycorrhizal *M. truncatula* roots, and recently
369 the rice ortholog *OsNPF4.5* was functionally characterized as an AM-induced nitrate
370 transporter (Wang et al. 2020). Overall, the stronger expression of ammonium and nitrate
371 transporters in Ri09- than in Ga165-colonized roots aligns with the observed increase in
372 the ^{15}N labeling in the shoots of Ri09-colonized plants.

373 The AM-induced P transporters *PT4* and *PT8* were both highly expressed in AM
374 colonized roots, especially Ri09-colonized roots (**Fig. 6E**). Similarly, colonization with
375 both fungi, but particularly with Ri09, caused an increase in shoot P content. However,
376 *Medtr1g074930*, a putative high affinity inorganic phosphate transporter, was strongly
377 upregulated in Ga165-colonized roots (**Fig. 6E**). This P transporter is upregulated during
378 P deficiency (Wang et al. 2017), and the upregulation of *Medtr1g074930* in our study
379 could indicate that colonization by Ga165 resulted in P deficiency in the host plant.
380 However, this is inconsistent with the observation that *Medtr1g074930* was not
381 upregulated in the roots of NM plants (**Fig. 6E**) and Ga165-colonized roots had a higher
382 P concentration than NM roots (**Supplemental Fig. S2**). Regardless, others have
383 similarly observed that the expression of high affinity P transporters are differentially
384 regulated in the host by colonization with different species of AM fungi (Grunwald et al.
385 2009).

386 Like N and P, AM fungi also play a critical role in supplying sulfur to the host plant
387 (Sieh et al. 2013). We observed an upregulation of two sulfate transporters, *SULTR1.1*
388 and *SULTR1.2* (**Fig. 6F**). Both are upregulated in mycorrhizal *M. truncatula* roots,

389 although not consistently (Casieri et al. 2012; Wipf et al. 2014). The *SULTR1.2* ortholog
390 in *Lotus japonicus* appears to play an important role in both direct and mycorrhizal sulfur
391 uptake pathways, and its promoter is active in arbuscule-containing cells (Giovannetti et
392 al. 2014). We also observed that the putative sulfate transporter gene *MOT1.1* was
393 upregulated in Ga165 and Ri09-colonized roots (**Fig. 6F**). However, the involvement of
394 MOT1.1 in sulfur transport has not been experimentally demonstrated yet, but it is
395 phylogenetically related to *MOT1.3*, which is a molybdate transporter crucial for the
396 rhizobia-legume symbiosis (Tejada-Jiménez et al. 2017).
397

398 **Patterns of photosynthesis, carbon transporter, and lipid biosynthesis gene**
399 **expression in the host plant are linked to the nutritional benefits provided by the**
400 **fungal symbiont**

401 In exchange for the nutritional benefits that AM fungi provide, plants transfer between 4
402 and 20% of their net fixed carbon in the form of carbohydrates and lipids to these fungal
403 symbionts (Wright et al. 1998; Roth and Paszkowski 2017). Both the nutritional benefits
404 that AM fungi provide and the increased carbon sink they create are known to stimulate
405 an increase in photosynthesis (Kaschuk et al. 2009). In line with this, we observed that
406 the expression levels of photosynthesis-related genes were more strongly induced in
407 Ri09- than in Ga165-colonized plants (**Fig. 8A**); thus, the elevated growth response
408 provided by Ri09 (**Fig. 2A-B**) was likely not only due to an increased nutrient transfer, but
409 potentially also due to a stimulation in photosynthesis.

410 Our previous studies have shown that host plants preferentially allocate more
411 carbon to the more cooperative AM fungus Ri09 (Kiers et al. 2011). Yet, we found that

412 the putative lipid transporters *STR* and *STR2* were upregulated in AM roots, but did not
413 differ significantly between Ga165 and Ri09-colonized roots (**Fig. 7C**). Nevertheless, we
414 did observe that the expression levels of the lipid biosynthesis gene *RAM2* (**Fig. 5**) and
415 the sugar transporter *SWEET1.2* (**Fig. 5F**) were higher in Ri09-colonized roots, which is
416 suggestive of increased transport of carbon resources to the fungus in exchange for
417 elevated nutritional benefits (Bravo et al. 2017; An et al. 2019).

418 Although *SWEET1.2* is highly upregulated during AM colonization, particularly in
419 arbusculated cortical cells, it is not essential for the maintenance of the AM symbiosis,
420 most likely because of functional redundancy between SWEET1.2 and other SWEETs
421 (An et al. 2019). We found that *SWEET3.3* and *SWEET12* were more strongly
422 upregulated in Ri09-colonized roots (**Fig. 7F**); both are upregulated in arbusculated
423 cortical cells in *M. truncatula* (Sameeullah et al. 2016). Interestingly, *SWEET7* and
424 *SWEET13* were more strongly induced in Ga165-colonized roots, but SWEETs perform
425 diverse physiological functions, and their upregulation does not necessarily increase
426 sugar transport to the fungus. For example, some SWEET transporters in *Arabidopsis*
427 localize to the tonoplast and restrict sugar efflux from the root (Chen et al. 2015). Given
428 the variable expression patterns of these five SWEETs in Ri09 and Ga165-colonized
429 roots and the varying roles they may play in sugar efflux and retention, functionally
430 characterizing them will improve our understanding of the mechanisms controlling carbon
431 allocation during AM symbioses.

432

433

434 **Arbuscular mycorrhiza-induced changes in the expression of host abiotic and**
435 **biotic stress response genes are species specific**

436 Although the primary focus of this study was to evaluate both resource exchange and
437 transporter expression, our gene expression data also provided some unique insights into
438 biotic and abiotic stress responses. Mycorrhizal growth responses are context-dependent
439 and fall along a mutualism to parasitism continuum (Johnson and Graham 2013). In
440 natural environments, plants are colonized by communities of AM fungi, which supports
441 the idea of functional complementarity, where a host plant experiences a broad range of
442 benefits that are provided by specific members of the AM fungal community (*e.g.*,
443 enhanced nutrient availability or increased disease resistance; Jansa et al., 2008). While
444 Ga165 does not seem to provide sufficient nutritional benefits to elicit a positive growth
445 response, it is possible that like other AM fungal species it may provide resistance to one
446 or more abiotic stresses (*e.g.*, salinity or heavy metal accumulation), none of which were
447 evaluated in this study.

448 We found that Ga165 more strongly up-regulated defense-response genes in the
449 shoots (**Fig. 8B**), two of which (*Medtr4g120760* and *Medtr8g096900*) are upregulated in
450 alfalfa when challenged with the foliar fungal pathogen *Phoma medicaginis* (Li et al.
451 2019a) and pea aphids (*Acyrthosiphon pisum*; Li et al., 2019b). There are two potential
452 explanations for this observation. The plant could show similar responses to a low benefit
453 AM fungus than to known fungal pathogens, or Ga165 could be more effective than Ri09
454 at priming host defense responses and thereby prevent infection from pathogens and
455 mitigating arthropod attack as previously been described for other AM fungal species (Liu
456 et al. 2007; Sharma et al. 2017).

457 Similarly, we also observed that genes associated with abiotic stress were
458 upregulated in Ga165-colonized roots (**Supplemental Fig. S6A)**. Three of these genes
459 — *Medtr5g063670*, *Medtr7g093170*, and *Medtr8g026960* — were very strongly
460 upregulated and are annotated as annexin D8, seed maturation protein, and homeobox
461 associated leucine zipper protein, respectively. Although the precise role of annexin D8
462 is not known, other annexins are differentially regulated during various abiotic and biotic
463 stresses, and some seem to play a role during AM symbiosis (Roux et al. 2012). The
464 seed maturation protein *Medtr7g093170* has been characterized as the late
465 embryogenesis abundant protein LEA1370, which is upregulated under various abiotic
466 stresses, including abscisic acid treatment, cold, salinity and dehydration (Zhang et al.
467 2020). Finally, the homeobox associated leucine zipper protein encoded by
468 *Medtr8g026960* was characterized as a transcription factor that is upregulated during salt
469 stress in alfalfa (Postnikova et al. 2013). However, since these genes are not yet
470 functionally characterized, the question whether Ga165 colonization could contribute to
471 an alleviation of these abiotic stresses, or whether host plants respond similarly to abiotic
472 stress and to Ga165 colonization, requires further studies.

473 It is also possible that Ga165 truly is a low-benefit symbiont capable of persisting
474 in a community with high benefit AM fungi thereby avoiding both detection and
475 subsequent sanctioning by the host plant for poor performance (Hart et al. 2013).
476 Avoiding detection could be carried out using effectors, as has been described in the
477 model AM fungus *R. irregularis* DAOM197198 that counteracts the plant immune program
478 with the small, secreted peptide SP7 (Kloppholz et al. 2011). Indeed, in our root
479 expression data we observed that 11 defense response genes, including three defensins

480 (*Medtr8g012810, Medtr8g012815*, and *Medtr8g012845*) were strongly up-regulated in
481 Ri09, but not in Ga165-colonized roots (**Supplemental Fig. S6B**, **Supplemental Table**
482 **S5**). Defensins are known to inhibit pathogen growth (Maróti et al. 2015), so it is tempting
483 to speculate that Ga165 could temper host defense responses to avoid detection and
484 sanctioning. However, the defensin *DefMd1* when overexpressed upregulates the
485 expression of the GRAS transcription factor *RAM1*, which plays a critical role in
486 arbuscular branching (Park et al., 2015; Uhe et al., 2018). *RAM1* was highly upregulated
487 in both Ga165 and Ri09 colonized roots (**Supplemental Table S3**) suggesting that
488 defensins might play a role in AM symbiosis.
489

490 **Transporter expression patterns in *Medicago truncatula* roots reveal interesting**
491 **candidates for future functional characterization**

492 This study has provided novel insights into the physiological and transcriptomic response
493 of a host plant to colonization by both high and low benefit AM fungi and **Fig. 9** provides
494 an overview of these responses. The experimental approach allowed us to identify both
495 the molecular mechanisms controlling the observed physiological responses and
496 transporters that are both commonly and uniquely regulated by high (Ri09) and low
497 benefit (Ga165) AM fungal species. While the primary focus of our study was on N, P,
498 and carbon transporters in the roots of *M. truncatula* colonized by Ga165 or Ri09, our
499 analysis of differentially expressed transporters uncovered some interesting gene
500 candidates with unique expression patterns (**Figs. 6** and **7**). Although there was a core
501 set of transporters similarly induced by both fungi, a smaller set were expressed
502 differently, and many are prime candidates for future functional analysis.

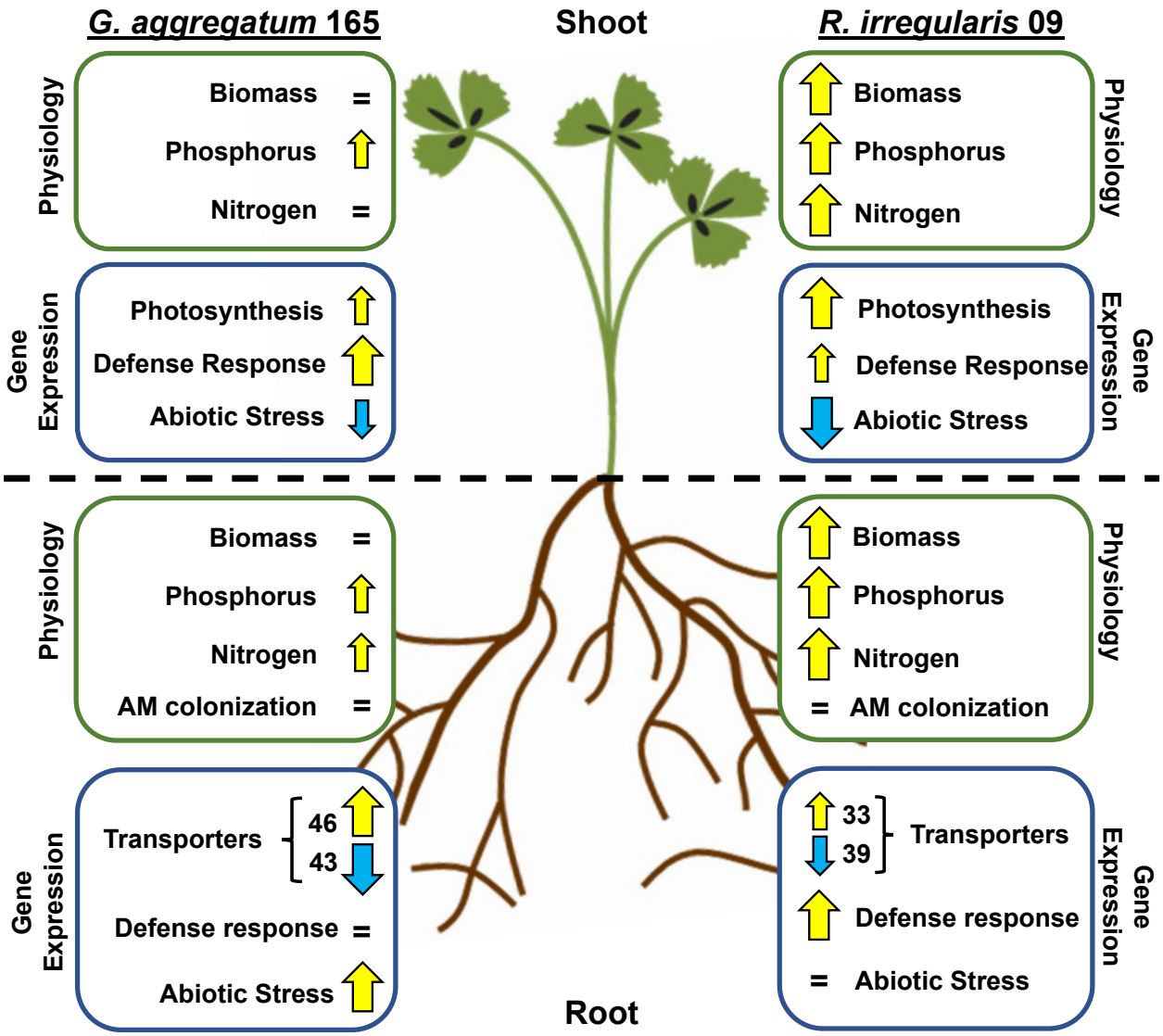

Figure 9. Summary of the physiological and transcriptomic responses in roots and shoots of *Medicago truncatula* colonized by either *Glomus aggregatum* 165 or *Rhizophagus irregularis* 09. Physiological data include the analysis of AM colonization, plant biomass, and both phosphorus and nitrogen-15 contents in plant tissues. Transcriptomic data include the expression patterns of nutrient transporters and enrichment of gene ontology terms. Yellow up-arrows indicate an increase, equal signs (=) specify no change, and blue down-arrows designate a decrease in each response compared to non-mycorrhizal plants. Arrow size indicates the degree of the response.

503 Multiple ABC transporters were induced by AM colonization (**Fig. 7C**), and two of
504 these, *STR* and *STR2*, have already been studied extensively (Zhang et al., 2010). Two
505 other transporters, *AMN2* and *AMN3*, are also well studied, but the substrate they
506 transport remains elusive (Roy et al. 2021). The two remaining genes, *Medtr4g124040*
507 and *Medtr1g050525*, have not been functionally characterized and could represent
508 interesting targets for future studies. The amino acid transporters *Medtr1g030660* and
509 *Medtr2g101920* and the peptide transporters *PTR3* and *OPT15* were all upregulated in
510 mycorrhizal roots. None of these have been functionally characterized, but the protein
511 product of *Medtr2g101920* was isolated from the plasma membrane of AM roots (Aloui et
512 al. 2018). Future characterization of these transporters will provide greater insight into the
513 extensive nutrient exchange mechanisms that support the AM symbiosis.
514 In conclusion, the comparison of the physiological and transcriptomic response of *M.*
515 *truncatula* to colonization with two AM fungal species that provide different nutritional
516 benefits to the host allowed us to identify some of the molecular mechanisms that control
517 reciprocal nutrient exchange. These include specific N and P transporters that have
518 already been functionally characterized (e.g., *AMT2;3*, *AMT2;5*, *NPF4.12*, *PT4,* and *PT8*)
519 and others that have not (e.g., NIP1;5). In addition, this study uncovered differential
520 expression of genes putatively involved in the allocation of carbon resources to AM fungi
521 depending on their nutritional benefit (e.g., *RAM2, SWEET1.2, SWEET3.3 and SWEET12*
522 were upregulated in Ri09-colonized roots, while *SWEET7* and *SWEET13* were
523 upregulated in Ga165-colonized roots). Root colonization with diverse fungal
524 communities that are composed of both low and high benefit fungi, allows the host plant
525 to choose among multiple trading partners, but also to take advantage of the diverse

526 benefits that fungi within this community can provide. The differential gene expression in
527 the roots and shoots after colonization with AM fungi that differ in the symbiotic benefit
528 that they provide, indicates that host plants are able to fine tune their response to different
529 fungi in their community.
530

531 **MATERIALS AND METHODS**

532 **Biological materials and growth conditions**

533 *M. truncatula* 'Jemalong A17' seeds were acid scarified in 36N H_2SO_4 (Fisher Scientific
534 Inc., Waltham, MA, USA), surface sterilized with 8.25% sodium hypochlorite (Clorox®
535 bleach, The Clorox Company, Oakland, CA, USA), rinsed with sterile Type 1 water and
536 imbibed at 4°C overnight. The seeds were then transferred onto moist autoclaved filter
537 paper in Petri dishes and kept in the dark for 3 d. Finally, the Petri dishes were placed in
538 ambient conditions for 7 d. Fully germinated seedlings were transferred into the root
539 compartment (RC) of a custom-made, two-compartment pot measuring 12 cm x 8 cm x 8
540 cm (L x W x H; **Supplemental Fig. S1**). The RC was separated from the hyphal
541 compartment (HC) by a 0.1 cm-thick plastic divider sealed on all sides by silicone
542 (Aqueon, Franklin, WI, USA). A hole in the middle of the divider (~3.12 cm in diameter)
543 was covered on both sides with a sheet of fine nylon mesh with 50 µm pores. Between
544 these sheets was a coarse nylon mesh with 1000 µm pores to create an air gap and inhibit
545 mass flow between the RC and the HC. This allowed fungal hyphae, but not roots, to
546 crossover from the RC to the HC (**Supplemental Fig. S1**). Both compartments were filled
547 with 250 ml of sterilized soil substrate containing 40% sand, 20% perlite, 20% vermiculite,
548 and 20% soil by volume. The soil substrate had an original concentration of 4.81 mg kg^{-1}

549 of Olsen's extractable phosphate, 10 mg kg^{-1} of NH_4^+, 34.4 mg kg^{-1} of NO_3^-, and a pH of
550 8.26. These nutrient levels were sufficiently low to induce host demand for N and P and
551 to stimulate AM colonization.

552 Fungal inoculum for *Rhizophagus irregularis* isolate 09 (Ri09; collected from
553 Southwest Spain by Mycovitro S.L. Biotechnología ecológica, Granada, Spain) and
554 *Glomus aggregatum* isolate 165 (Ga165; collected from the Long Term Mycorrhizal
555 Research Site, University of Guelph, Canada) were produced using axenic root organ
556 cultures of Ri T-DNA transformed carrot (*Daucus carota* clone DCI) grown on minimal
557 medium (St-Arnaud et al. 1996). After approximately eight weeks of growth, spores were
558 isolated by blending the medium in 10 mM citrate buffer (pH 6.0). Then, at transplanting,
559 each seedling was inoculated with ~0.4 g mycorrhizal roots and ~500 spores of either
560 Ri09 or Ga165. Non-mycorrhizal (NM) controls received a similar quantity of double
561 autoclaved roots and spores. After transplanting and fungal inoculation, the plants were
562 grown in a growth chamber (model TC30; Conviron, Winnipeg, MB, Canada) with a 25°C
563 day/20°C night cycle, 30% relative humidity, and a photosynthetic photon flux of ~225
564 μmol m^{-2} s^{-1}.

565

566 **Experimental design**

567 Throughout the experiment, the position of the plants within the growth chamber was
568 randomized three times. Five weeks post-inoculation, 4 mM $^{15}NH_4Cl$ (Sigma Aldrich, St.
569 Louis, USA) and 0.5 mM KH_2PO_4 were added to the HC of colonized and noncolonized
570 plants in a modified Ingestad solution (Ingestad 1960). The plants were harvested two
571 weeks later (seven weeks post-inoculation).

572 **Biomass determination, mycorrhizal quantification, and analysis of nitrogen and**
573 **phosphorus contents in plants**

574 At plant harvest, shoots and roots were separated to determine their respective fresh
575 weight. Subsamples of both tissues were flash frozen in liquid N_2 and stored at -80°C for
576 transcriptome analysis. An additional root subsample was collected and stored in 50%
577 ethanol at 4°C to assess AM colonization. The remaining plant tissue was dried at 70°C
578 for 48 h and then shoot and root dry weights were recorded. To determine the level of AM
579 colonization, the root samples were cleared with 10% KOH at 80°C for 30 min, rinsed with
580 tap water, and stained with 5% Sheaffer ink-vinegar (v:v) at 80°C for 15 min (Vierheilig et
581 al. 1998). Total AM colonization rates were assessed using the gridline intersection
582 method (McGonigle et al. 1990). We did not observe any fungal structures in the roots of
583 NC control plants. Subsamples of dried shoot and root tissues were pulverized using a
584 tissue homogenizer (Precellys 24 Dual, Cayman Chemical Company, Ann Arbor, MI,
585 USA) and digested with 2N HCl for 2 h at 95°C. The P concentration in the plant tissues
586 was spectrophotometrically determined at 436 nm after adding ammonium molybdate
587 vanadate solution (Fisher Scientific, Pittsburgh, USA). Measurements of nitrogen-15 in
588 plant tissues were performed by quantitative NMR spectroscopy as described previously
589 (Kafle et al. 2018).

590

591 **Fluorescent staining and confocal analysis of arbuscules**

592 Ink-stained roots that contained arbuscules were subsequently stained for confocal
593 imaging as described in Cope et al. (2019). Briefly, they were incubated overnight at 4°C
594 in 1X PBS containing 2 µg ml^{-1} Alexa Fluor 488™ conjugated to wheat germ agglutinin

595 (WGA; Thermo Fischer Scientific, Waltham, MA, USA). The next day, stained roots were
596 rinsed with 1X PBS, mounted on a glass slide, and immediately observed on an Olympus
597 FV1200 confocal laser scanning microscope (Olympus, Shinjuku, Tokyo, Japan) with an
598 Olympus UPlanApo 40×/0.85 objective. The emission spectra of Alexa Fluor 488™ WGA
599 (500 to 540 nm) was detected after excitation with a 488-nm laser. Other settings used in
600 the Fluoview v4.2c acquisition software (*e.g.*, laser intensity, gain, offset, magnification,
601 airy units) were similar for all sample observations. The width of 488 and 508 arbuscules
602 from 22 Ga165 and 21 Ri09-colonized root segments, respectively, were measured using
603 Fiji (Schindelin et al. 2012).
604
605 **RNA sequencing and analysis**
606 Root and shoot tissues from four biological replicates (n = 4) were homogenized in liquid
607 N2, and total RNA was extracted using the PureLinkTM RNA Mini Kit (Thermo Fisher
608 Scientific). Extracted RNA was treated with TURBO™ DNase (Thermo Fisher Scientific)
609 and quantified using a NanoDrop ND-2000 spectrophotometer (Thermo Fisher Scientific).
610 RNA quality was assessed using 2100 BioAnalyzer technology (Agilent Technologies).
611 Approximately 100 ng of total RNA was used to construct poly(A) selection libraries using
612 the Illumina TruSeq RNA Sample Preparation kit and 150-nucleotide single-end reads
613 were sequenced using an Illumina NextSeq500 with high output flow cells (Genomics
614 Sequencing Facility, South Dakota State University).
615 The RNA sequencing data were uploaded to Discovery Environment
616 (https://de.cyverse.org/de) and read quality of each fastq file was evaluated using FastQC
617 0.11.5 (https://www.bioinformatics.babraham.ac.uk/projects/fastqc/). One Ga165 and

618 one NC root sample and one Ri09 shoot sample were discarded due to poor quality. The
619 remaining root (n=3, Ga165 and NC; n=4, Ri09) and shoot (n=4, Ga165 and NC; n=3,
620 Ri09) samples were aligned to the reference genome of *M. truncatula* 'Jemalong A17'
621 (JCVI Mt4.0; Tang et al., 2014) using HISAT2.1 (Kim et al. 2019). Aligned reads were
622 then assembled and merged using StringTie-1.3.3 (Pertea et al. 2015) and the *M.*
623 *truncatula* JCVI 4.0v2 annotation file (Tang et al. 2014). Finally, Cuffdiff2.1.1 (Trapnell et
624 al. 2013) was used to quantify transcript abundance. The output files from CuffDiff2.1.1
625 were visualized in R v3.6.2 (The R Foundation 2020) using the CummeRbund package
626 (Goff et al. 2012). For further analyses, the differential gene expression output files from
627 CuffDiff2.1.1 were imported into Microsoft Excel (Microsoft 365®) and sorted to identify
628 significantly differentially expressed genes (DEGs) with a log2 fold-change > 2 and a false
629 discovery rate-adjusted q-value < 0.05. All DEGs outside this threshold were not
630 considered for further analysis. Venn diagrams of DEGs were generated using the
631 Bioinformatics & Evolutionary Genomics Web tool
632 (http://bioinformatics.psb.ugent.be/webtools/Venn/) and heatmaps of FPKM (Fragments
633 Per Kilobase of transcript per Million mapped reads) values from all DEGs across
634 inoculation regimes were generated using Cluster 3.0 and Java TreeView
635 (http://bonsai.hgc.jp/~mdehoon/software/cluster/software.htm). Gene ontology (GO)
636 enrichment analysis was conducted with the web-based tool PlantTFDB 4.0
637 (http://plantregmap.gao-lab.org/go.php).
638
639

640 **Statistical analysis**

641 For the physiological response variables, unless mentioned otherwise, mean and
642 standard error of the mean were determined from five independent biological replicates
643 for each colonization regime, including noncolonized and either Ga165 or Ri09-colonized
644 plants. One-way ANOVA was used to identify statistically significant differences ($p \leq 0.05$)
645 among all three colonization regimes for dry weight, P concentration, P content, and
646 nitrogen-15 enrichment. The least significant difference (LSD) test was subsequently
647 used for pairwise multiple comparisons to identify significant differences ($p \leq 0.05$) among
648 treatments. These statistical analyses were conducted using Statistix 9 (analytical
649 software, Tallahassee, FL, USA). For AM colonization and arbuscule size, statistically
650 significant differences ($p \leq 0.05$) between the Ga165 and Ri09 mycorrhizal treatments
651 were determined using a Welch's two-sample t-test in R v4.0.2 (The R Foundation 2020).
652 Only results that are significant at the $p \leq 0.05$-level are primarily discussed. All F statistics
653 and p-values are shown in **Supplemental Table S1**.

654

655 **ACKNOWLEDGEMENTS**

656 This work was funded by the USDA (2017-67014-26530), the SD Soybean Research and
657 Promotion Council, and the Agricultural Experiment Station at SDSU to HK and SS. KG
658 acknowledges support of the North Carolina Agriculture Research Service (NCARS), the
659 North Carolina Soybean Producers Association (2019-1656), and the USDA (2020-
660 67013-31800). We would like to thank Lindsay McKeever for performing the Kjeldahl
661 degradations for the $^{15}N/^{14}N$ analyses.

662

663 **LITERATURE CITED**

664 Aloui, A., Recorbet, G., Lemaître-Guillier, C., Mounier, A., Balliau, T., Zivy, M., Wipf, D.,
665 and Dumas-Gaudot, E. 2018. The plasma membrane proteome of *Medicago*
666 *truncatula* roots as modified by arbuscular mycorrhizal symbiosis. Mycorrhiza.
667 28:1–16

668 An, J., Zeng, T., Ji, C., de Graaf, S., Zheng, Z., Xiao, T. T., Deng, X., Xiao, S., Bisseling,
669 T., Limpens, E., and Pan, Z. 2019. A *Medicago truncatula* SWEET transporter
670 implicated in arbuscule maintenance during arbuscular mycorrhizal symbiosis. New
671 Phytol. 224:396–408

672 Besserer, A., Becard, G., Jauneau, A., Roux, C., Sejalon-Delmas, N., Bécard, G.,
673 Jauneau, A., Roux, C., and Séjalon-Delmas, N. 2008. GR24, a synthetic analog of
674 strigolactones, stimulates the mitosis and growth of the abuscular mycorrhizal
675 fungus *Gigaspora rosea* by boosting its energy metabolism. Plant Physiol.
676 148:402–413

677 Bravo, A., Brands, M., Wewer, V., Dörmann, P., and Harrison, M. J. 2017. Arbuscular
678 mycorrhiza-specific enzymes FatM and RAM2 fine-tune lipid biosynthesis to
679 promote development of arbuscular mycorrhiza. New Phytol. 214:1631–1645

680 Breuillin-Sessoms, F., Floss, D. S., Karen Gomez, S., Pumplin, N., Ding, Y., Levesque-
681 Tremblay, V., Noar, R. D., Daniels, D. A., Bravo, A., Eaglesham, J. B., Benedito, V.
682 A., Udvardi, M. K., Harrison, M. J., Gomez, S. K., Pumplin, N., Ding, Y., Levesque-
683 Tremblay, V., Noar, R. D., Daniels, D. A., Bravo, A., Eaglesham, J. B., Benedito, V.
684 A., Udvardi, M. K., Harrison, M. J., Karen Gomez, S., Pumplin, N., Ding, Y.,
685 Levesque-Tremblay, V., Noar, R. D., Daniels, D. A., Bravo, A., Eaglesham, J. B.,

686 Benedito, V. A., Udvardi, M. K., and Harrison, M. J. 2015. Suppression of arbuscule
687 degeneration in *Medicago truncatula* phosphate transporter4 mutants is dependent
688 on the ammonium transporter 2 family protein AMT2;3. Plant Cell. 27:1352–1366
689 Brundrett, M. C., and Tedersoo, L. 2018. Evolutionary history of mycorrhizal symbioses
690 and global host plant diversity. New Phytol. 220:1108–1115
691 Bücking, H., and Kafle, A. 2015. Role of arbuscular mycorrhizal fungi in the nitrogen
692 uptake of plants: Current knowledge and research gaps. Agronomy. 5:587–612
693 Casieri, L., Gallardo, K., and Wipf, D. 2012. Transcriptional response of *Medicago*
694 *truncatula* sulphate transporters to arbuscular mycorrhizal symbiosis with and
695 without sulphur stress. Planta. 235:1431–1447
696 Chandrasekaran, M. 2020. A meta-analytical approach on arbuscular mycorrhizal fungi
697 inoculation efficiency on plant growth and nutrient uptake. Agriculture. 10:370
698 Chen, H. Y., Huh, J. H., Yu, Y. C., Ho, L. H., Chen, L. Q., Tholl, D., Frommer, W. B.,
699 and Guo, W. J. 2015. The Arabidopsis vacuolar sugar transporter SWEET2 limits
700 carbon sequestration from roots and restricts *Pythium* infection. Plant J. 83:1046–
701 1058
702 Cope, K. R., Bascaules, A., Irving, T. B., Venkateshwaran, M., Maeda, J., Garcia, K.,
703 Rush, T. A., Ma, C., Labbé, J., Jawdy, S., Steigerwald, E., Setzke, J., Fung, E.,
704 Schnell, K. G., Wang, Y., Schleif, N., Bücking, H., Strauss, S. H., Maillet, F.,
705 Jargeat, P., Bécard, G., Puech-Pagès, V., and Ané, J.-M. M. 2019. The
706 ectomycorrhizal fungus *Laccaria bicolor* produces lipochitooligosaccharides and
707 uses the common symbiosis pathway to colonize populus roots. Plant Cell.
708 31:2386–2410

709 Davière, J. M., and Achard, P. 2013. Gibberellin signaling in plants. Development.
710 140:1147–1151
711 Doidy, J., Vidal, U., and Lemoine, R. 2019. Sugar transporters in Fabaceae, featuring
712 SUT MST and SWEET families of the model plant *Medicago truncatula* and the
713 agricultural crop *Pisum sativum* J.J. Zwiazek, ed. PLoS One. 14:e0223173
714 Fellbaum, C. R., Mensah, J. A., Cloos, A. J., Strahan, G. E., Pfeffer, P. E., Kiers, E. T.,
715 and Bücking, H. 2014. Fungal nutrient allocation in common mycorrhizal networks
716 is regulated by the carbon source strength of individual host plants. New Phytol.
717 203:646–656
718 Floss, D. S., Levy, J. G., Lévesque-Tremblay, V., Pumplin, N., and Harrison, M. J. 2013.
719 DELLA proteins regulate arbuscule formation in arbuscular mycorrhizal symbiosis.
720 Proc. Natl. Acad. Sci. U. S. A. 110:E5025-34
721 Frare, R., Ayub, N., Alleva, K., and Soto, G. 2018. The ammonium channel NOD26 is
722 the evolutionary innovation that drives the emergence, consolidation, and
723 dissemination of nitrogen-fixing symbiosis in angiosperms. J. Mol. Evol. 86:554–
724 565
725 Garcia, K., Doidy, J., Zimmermann, S. D., Wipf, D., and Courty, P. E. 2016. Take a trip
726 through the plant and fungal transportome of mycorrhiza. Trends Plant Sci. 21:937–
727 950
728 Genre, A., Chabaud, M., Balzergue, C., Puech-Pagès, V., Novero, M., Rey, T.,
729 Fournier, J., Rochange, S., Bécard, G., Bonfante, P., and Barker, D. G. 2013.
730 Short-chain chitin oligomers from arbuscular mycorrhizal fungi trigger nuclear Ca^{2+}
731 spiking in *Medicago truncatula* roots and their production is enhanced by

732 strigolactone. New Phytol. 198:190–202
733 Giovannetti, M., Tolosano, M., Volpe, V., Kopriva, S., and Bonfante, P. 2014.
734 Identification and functional characterization of a sulfate transporter induced by
735 both sulfur starvation and mycorrhiza formation in *Lotus japonicus*. New Phytol.
736 204:609–619
737 Goff, L. A., Trapnell, C., and Kelley, D. 2012. CummeRbund: visualization and
738 exploration of Cufflinks high-throughput sequencing data. R Packag. version. 2:1–
739 45
740 Grunwald, U., Guo, W., Fischer, K., Isayenkov, S., Ludwig-Müller, J., Hause, B., Yan,
741 X., Küster, H., and Franken, P. 2009. Overlapping expression patterns and
742 differential transcript levels of phosphate transporter genes in arbuscular
743 mycorrhizal, Pi-fertilised and phytohormone-treated *Medicago truncatula* roots.
744 Planta. 229:1023–1034
745 Hart, M. M., Forsythe, J., Oshowski, B., Bücking, H., Jansa, J., and Kiers, E. T. 2013.
746 Hiding in a crowd - Does diversity facilitate persistence of a low-quality fungal
747 partner in the mycorrhizal symbiosis? Symbiosis. 59:47–56
748 Havlin, J. L., Beaton, J. D., Tisdale, S. L., and Nelson, W. L. 2014. *Soil Fertility and*
749 *Fertilizers: An Introduction to Nutrient Management*. Eighth. Pearson Education,
750 Inc.
751 Ingestad, T. 1960. Studies on the nutrition of forest tree seedlings. III mineral nutrition of
752 pine. Physiol. Plant. 13:513–533
753 Jansa, J., Smith, F. A., and Smith, S. E. 2008. Are there benefits of simultaneous root
754 colonization by different arbuscular mycorrhizal fungi? New Phytol. 177:779–789

755 Javot, H., Penmetsa, R. V., Terzaghi, N., Cook, D. R., and Harrison, M. J. 2007. A
756 *Medicago truncatula* phosphate transporter indispensable for the arbuscular
757 mycorrhizal symbiosis. Proc. Natl. Acad. Sci. 104:1720–1725
758 Johnson, N. C., and Graham, J. H. 2013. The continuum concept remains a useful
759 framework for studying mycorrhizal functioning. Plant Soil. 363:411–419
760 Kafle, A., Cope, K. R., Raths, R., Yakha, J. K., Subramanian, S., Bücking, H., and
761 Garcia, K. 2019. Harnessing soil microbes to improve plant phosphate efficiency in
762 cropping systems. Agronomy. 9:127
763 Kafle, A., Garcia, K., Wang, X., Pfeffer, P. E., Strahan, G. D., and Bücking, H. 2018.
764 Nutrient demand and fungal access to resources control the carbon allocation to
765 the symbiotic partners in tripartite interactions of *Medicago truncatula*. Plant. Cell
766 Environ. :1–15
767 Kaschuk, G., Kuyper, T. W., Leffelaar, P. A., Hungria, M., and Giller, K. E. 2009. Are the
768 rates of photosynthesis stimulated by the carbon sink strength of rhizobial and
769 arbuscular mycorrhizal symbioses? Soil Biol. Biochem. 41:1233–1244
770 Kiers, E. T., Duhamel, M., Beesetty, Y., Mensah, J. a, Franken, O., Verbruggen, E.,
771 Fellbaum, C. R., Kowalchuk, G. A., Hart, M. M., Bago, A., Palmer, T. M., West, S.
772 a, Vandenkoornhuyse, P., Jansa, J., Bücking, H., and Bucking, H. 2011. Reciprocal
773 rewards stabilize cooperation in the mycorrhizal symbiosis. Science (80-.).
774 333:880–882
775 Kim, D., Paggi, J. M., Park, C., Bennett, C., and Salzberg, S. L. 2019. Graph-based
776 genome alignment and genotyping with HISAT2 and HISAT-genotype. Nat.
777 Biotechnol. 37:907–915

778 Kloppholz, S., Kuhn, H., and Requena, N. 2011. A secreted fungal effector of *Glomus*
779 *intraradices* promotes symbiotic biotrophy. Curr. Biol. 21:1204–1209
780 Kretzschmar, T., Kohlen, W., Sasse, J., Borghi, L., Schlegel, M., Bachelier, J. B.,
781 Reinhardt, D., Bours, R., Bouwmeester, H. J., and Martinoia, E. 2012. A petunia
782 ABC protein controls strigolactone-dependent symbiotic signalling and branching.
783 Nature. 483:341–344
784 LeBauer, D. S., and Treseder, K. K. 2008. Nitrogen limitation of net primary productivity
785 in terrestrial ecosystems is globally distributed. Ecology. 89:371–379
786 Li, Y., Duan, T., Nan, Z., and Li, Y. 2019a. Arbuscular mycorrhizal fungus alleviates
787 alfalfa leaf spots caused by *Phoma medicaginis* revealed by RNA-seq analysis. J.
788 Appl. Microbiol. :jam.14387
789 Li, Y., Nan, Z., and Duan, T. 2019b. *Rhizophagus intraradices* promotes alfalfa
790 (*Medicago sativaM*) defense against pea aphids (*Acyrthosiphon pisum*) revealed by
791 RNA-Seq analysis. Mycorrhiza. 29:623–635
792 Liu, J., Maldonado-Mendoza, I., Lopez-Meyer, M., Cheung, F., Town, C. D., and
793 Harrison, M. J. 2007. Arbuscular mycorrhizal symbiosis is accompanied by local
794 and systemic alterations in gene expression and an increase in disease resistance
795 in the shoots. Plant J. 50:529–544
796 MacLean, A. M., Bravo, A., and Harrison, M. J. 2017. Plant signaling and metabolic
797 pathways enabling arbuscular mycorrhizal symbiosis. Plant Cell. 29:2319–2335
798 Maillet, F., Poinsot, V., André, O., Puech-Pagés, V., Haouy, A., Gueunier, M., Cromer,
799 L., Giraudet, D., Formey, D., Niebel, A., Martinez, E. A., Driguez, H., Bécard, G.,
800 and Dénarié, J. 2011. Fungal lipochitooligosaccharide symbiotic signals in

801 arbuscular mycorrhiza. Nature. 469:58–64
802 Maróti, G., Downie, J. A., and Kondorosi, É. 2015. Plant cysteine-rich peptides that
803 inhibit pathogen growth and control rhizobial differentiation in legume nodules.
804 Curr. Opin. Plant Biol. 26:57–63
805 Martin, F. M., Uroz, S., and Barker, D. G. 2017. Ancestral alliances: Plant mutualistic
806 symbioses with fungi and bacteria. Science (80-.). 356:eaad4501
807 McGonigle, T. P., Miller, M. H., Evans, D. G., Fairchild, G. L., and Swan, J. A. 1990. A
808 new method which gives an objective measure of colonization of roots by vesicular-
809 arbuscular mycorrhizal fungi. New Phytol. 115:495–501
810 Nadal, M., Sawers, R., Naseem, S., Bassin, B., Kulicke, C., Sharman, A., An, G., An, K.,
811 Ahern, K. R., Romag, A., Brutnell, T. P., Gutjahr, C., Geldner, N., Roux, C.,
812 Martinoia, E., Konopka, J. B., and Paszkowski, U. 2017. An N-acetylglucosamine
813 transporter required for arbuscular mycorrhizal symbioses in rice and maize. Nat.
814 Plants. 3:1–7
815 Nouri, E., Surve, R., Bapaume, L., Stumpe, M., Chen, M., Zhang, Y., Ruyter-Spira, C.,
816 Bouwmeester, H., Glauser, G., Bruisson, S., and Reinhardt, D. 2021. Phosphate
817 Suppression of Arbuscular Mycorrhizal Symbiosis Involves Gibberellic Acid
818 Signaling. Plant Cell Physiol.
819 Park, H.-J., Floss, D. S., Levesque-Tremblay, V., Bravo, A., and Harrison, M. J. 2015.
820 Hyphal branching during arbuscule development requires RAM1. Plant Physiol.
821 169:pp.01155.2015
822 Pertea, M., Pertea, G. M., Antonescu, C. M., Chang, T. C., Mendell, J. T., and Salzberg,
823 S. L. 2015. StringTie enables improved reconstruction of a transcriptome from

824 RNA-seq reads. Nat. Biotechnol. 33:290–295
825 Pimprikar, P., and Gutjahr, C. 2018. Transcriptional Regulation of Arbuscular
826 Mycorrhiza Development. Plant Cell Physiol. 59:673–690
827 Postnikova, O. A., Shao, J., and Nemchinov, L. G. 2013. Analysis of the alfalfa root
828 transcriptome in response to salinity stress. Plant Cell Physiol. 54:1041–1055
829 Roth, R., and Paszkowski, U. 2017. Plant carbon nourishment of arbuscular mycorrhizal
830 fungi. Curr. Opin. Plant Biol. 39:50–56
831 Roux, S. J., Clark, G. B., Morgan, R. O., Fernandez, M.-P. P., and Roux, S. J. 2012.
832 Evolutionary adaptation of plant annexins has diversified their molecular structures,
833 interactions and functional roles. New Phytol. 196:695–712
834 Roy, S. 2015. Analysis of gene expression, regulation, and function of three symbiotic
835 ABC subfamily-B transporters in *Medicago truncatula*.
836 Roy, S., Breakspear, A., Cousins, D., Torres-Jerez, I., Jackson, K. J., Kumar, A., Su, Y.,
837 Krom, N., Liu, C.-W., Udvardi, M., Xu, P., and Murray, J. D. 2021. Three common
838 symbiotic ABC-B transporters in Medicago truncatula are regulated by a NIN-
839 independent branch of the symbiosis signalling pathway. Mol. Plant-Microbe
840 Interact.
841 Rush, T. A., Puech-Pagès, V., Bascaules, A., Jargeat, P., Maillet, F., Haouy, A., Maës,
842 A. Q. M., Carriel, C. C., Khokhani, D., Keller-Pearson, M., Tannous, J., Cope, K. R.,
843 Garcia, K., Maeda, J., Johnson, C., Kleven, B., Choudhury, Q. J., Labbé, J., Swift,
844 C., O'Malley, M. A., Bok, J. W., Cottaz, S., Fort, S., Poinsot, V., Sussman, M. R.,
845 Lefort, C., Nett, J., Keller, N. P., Bécard, G., and Ané, J. M. 2020. Lipo-
846 chitooligosaccharides as regulatory signals of fungal growth and development. Nat.

847 Commun. 11:1–10
848 Sameeullah, M., Demiral, T., Aslam, N., Baloch, F. S., and Gurel, E. 2016. In silico
849 functional analyses of SWEETs reveal cues for their role in AMF symbiosis. Pages
850 45–58 in: Plant, Soil and Microbes: Volume 2: Mechanisms and Molecular
851 Interactions, Springer International Publishing.
852 Schindelin, J., Arganda-Carreras, I., Frise, E., Kaynig, V., Longair, M., Pietzsch, T.,
853 Preibisch, S., Rueden, C., Saalfeld, S., Schmid, B., Tinevez, J. Y., White, D. J.,
854 Hartenstein, V., Eliceiri, K., Tomancak, P., and Cardona, A. 2012. Fiji: An open-
855 source platform for biological-image analysis. Nat. Methods. 9:676–682
856 Sharma, E., Anand, G., and Kapoor, R. 2017. Terpenoids in plant and arbuscular
857 mycorrhiza-reinforced defence against herbivorous insects. Ann. Bot. 119:791–801
858 Sieh, D., Watanabe, M., Devers, E. A., Brueckner, F., Hoefgen, R., and Krajinski, F.
859 2013. The arbuscular mycorrhizal symbiosis influences sulfur starvation responses
860 of Medicago truncatula. New Phytol. 197:606–616
861 Spatafora, J. W., Chang, Y., Benny, G. L., Lazarus, K., Smith, M. E., Berbee, M. L.,
862 Bonito, G., Corradi, N., Grigoriev, I., Gryganskyi, A., James, T. Y., O'Donnell, K.,
863 Roberson, R. W., Taylor, T. N., Uehling, J., Vilgalys, R., White, M. M., and Stajich,
864 J. E. 2016. A phylum-level phylogenetic classification of zygomycete fungi based
865 on genome-scale data. Mycologia. 108:1028–1046
866 St-Arnaud, M., Hamel, C., Vimard, B., Caron, M., and Fortin, J. A. 1996. Enhanced
867 hyphal growth and spore production of the arbuscular mycorrhizal fungus Glomus
868 intraradices in an in vitro system in the absence of host roots. Mycol. Res.
869 100:328–332

870 Tang, H., Krishnakumar, V., Bidwell, S., Rosen, B., Chan, A., Zhou, S., Gentzbittel, L.,
871 Childs, K. L., Yandell, M., Gundlach, H., Mayer, K. F. X., Schwartz, D. C., and
872 Town, C. D. 2014. An improved genome release (version Mt4.0) for the model
873 legume Medicago truncatula. BMC Genomics. 15:312
874 Tejada-Jiménez, M., Gil-Díez, P., León-Mediavilla, J., Wen, J., Mysore, K. S., Imperial,
875 J., and González-Guerrero, M. 2017. *Medicago truncatula* Molybdate Transporter
876 type 1 (MtMOT1.3) is a plasma membrane molybdenum transporter required for
877 nitrogenase activity in root nodules under molybdenum deficiency. New Phytol.
878 216:1223–1235
879 The R Foundation. 2020. R: The R Project for Statistical Computing. Available at:
880 https://www.r-project.org/ [Accessed May 11, 2020].
881 Trapnell, C., Hendrickson, D. G., Sauvageau, M., Goff, L., Rinn, J. L., and Pachter, L.
882 2013. Differential analysis of gene regulation at transcript resolution with RNA-seq.
883 Nat. Biotechnol. 31:46–53
884 Uhe, M., Hogekamp, C., Hartmann, R. M., Hohnjec, N., and Küster, H. 2018. The
885 mycorrhiza-dependent defensin MtDefMd1 of *Medicago truncatula* acts during the
886 late restructuring stages of arbusculecontaining cells. PLoS One. 13:e0191841
887 Vernié, T., Camut, S., Camps, C., Rembliere, C., Carvalho-Niebel, F., Mbengue, M.,
888 Timmers, T., Gasciolli, V., Thompson, R., Le Signor, C., Lefebvre, B., Cullimore, J.,
889 and Hervé, C. 2016. PUB1 interacts with the receptor kinase DMI2 and negatively
890 regulates rhizobial and arbuscular mycorrhizal symbioses through its ubiquitination
891 activity in *Medicago truncatula*. Plant Physiol. 170:2312–2324
892 Vierheilig, H., Coughlan, A. P., Wyss, U., and Piché, Y. 1998. Ink and vinegar, a simple

893 staining technique for arbuscular-mycorrhizal fungi. Appl. Environ. Microbiol.
894 64:5004–5007
895 Vitousek, P. M., Porder, S., Houlton, B. Z., and Chadwick, O. A. 2010. Terrestrial
896 phosphorus limitation: mechanisms, implications, and nitrogen–phosphorus
897 interactions. Ecol. Appl. 20:5–15
898 Wang, S., Chen, A., Xie, K., Yang, X., Luo, Z., Chen, J., Zeng, D., Ren, Y., Yang, C.,
899 Wang, L., Feng, H., López-Arredondo, D. L., Herrera-Estrella, L. R., and Xu, G.
900 2020. Functional analysis of the OsNPF4.5 nitrate transporter reveals a conserved
901 mycorrhizal pathway of nitrogen acquisition in plants. Proc. Natl. Acad. Sci. U. S. A.
902 Wang, T., Zhao, M., Zhang, X., Liu, M., Yang, C., Chen, Y., Chen, R., Wen, J., Mysore,
903 K. S., and Zhang, W. H. 2017. Novel phosphate deficiency-responsive long non-
904 coding RNAs in the legume model plant *Medicago truncatula*. J. Exp. Bot. 68:5937–
905 5948
906 Wang, X., Zhao, S., and Bücking, H. 2016. Arbuscular mycorrhizal growth responses
907 are fungal specific but do not differ between soybean genotypes with different
908 phosphate efficiency. Ann. Bot. 118:11–21
909 Wipf, D., Mongelard, G., van Tuinen, D., Gutierrez, L., and Casieri, L. 2014.
910 Transcriptional responses of *Medicago truncatula* upon sulfur deficiency stress and
911 arbuscular mycorrhizal symbiosis. Front. Plant Sci. 5:680
912 Wright, D. P., Read, D. J., and Scholes, J. D. 1998. Mycorrhizal sink strength influences
913 whole plant carbon balance of Trifolium repens L. Plant, Cell Environ. 21:881–891
914 Yoneyama, K., Yoneyama, K., Takeuchi, Y., and Sekimoto, H. 2007. Phosphorus
915 deficiency in red clover promotes exudation of orobanchol, the signal for

916 mycorrhizal symbionts and germination stimulant for root parasites. Planta.
917 225:1031–1038
918 Zhang, Q., Blaylock, L. A., and Harrison, M. J. 2010. Two *Medicago truncatula* half-ABC
919 transporters are essential for arbuscule development in arbuscular mycorrhizal
920 symbiosis. Plant Cell. 22:1483–1497
921 Zhang, Y. M., Wang, H. Q., Liu, D. M., and Liu, R. J. 2020. Three tandemly aligned lea
922 genes from *Medicago truncatula* confer differential protection to *Escherichia coli*
923 against abiotic stresses. Biol. Plant. 64:95–103
924

925 **FIGURE LEGENDS**

926 **Figure 1.** Arbuscular mycorrhizal colonization of *Medicago truncatula* roots and arbuscule
927 size. **A,** percent root length colonization of roots inoculated with *Glomus aggregatum* 165
928 (Ga165; grey) or *Rhizophagus irregularis* 09 (Ri09; dark grey), measured for intraradical
929 hyphae (IRH), arbuscules, and vesicles. Data points represent individual values for
930 biological replicates (n = 5) and bars represent the mean ± SEM. **B-C**, representative
931 confocal microscope images of Ga165 (**B**) and Ri09 (**C**) arbuscules stained with wheat
932 germ agglutinin conjugated to Alexa Fluor 488. Scale bars = 50 µm. **D**, violin plot of
933 arbuscule widths measured in roots colonized by Ga165 (grey) or Ri09 (dark grey)
934 overlayed with box and whisker plots. In total, 488 and 508 arbuscules were measured in
935 Ga165 and Ri09-colonized roots, respectively. All data were analyzed using a Welch's
936 two-sample t-test and statistically significant differences ($p \leq 0.05$) are indicated with an
937 asterisk.
938

939 **Figure 2.** Biomass and nutrient content of *Medicago truncatula* plants colonized by
940 different arbuscular mycorrhizal fungi. Shown are dry weight (**A**,**B**), phosphorus content
941 (**C**,**D**), and % nitrogen-15 enrichment (**E**,**F**) of roots (left) and shoots (right). The plants
942 were inoculated with either *Glomus aggregatum* 165 (Ga165) or *Rhizophagus irregularis*
943 09 (Ri09) and compared to non-mycorrhizal (NM) control plants. Data points represent
944 individual values for biological replicates (n = 5) and bars represent the mean of each
945 treatment ± SEM. Different letters on the bars indicate statistically significant ($p \leq 0.05$)
946 differences based on one-way ANOVA and LSD test. F statistics and p-values are shown
947 in **Supplemental Table S1**.
948
949 **Figure 3.** Significantly differentially expressed genes in roots (**A–C**) and shoots (**D–F**) of
950 *Medicago truncatula* colonized by different AM fungi. **A** and **D**, Number of significantly
951 differentially expressed genes (DEGs; $\log_2$[fold-change] > 2 and a q-value < 0.05) in
952 plants colonized by *Glomus aggregatum* 165 (Ga165) or *Rhizophagus irregularis* 09
953 (Ri09) compared either to non-mycorrhizal (NM) control plants or to each other. **B** and **E**,
954 Venn diagrams of significantly upregulated (yellow) and downregulated (blue) DEGs
955 unique to Ga165 and Ri09-colonized plants or shared by both. **C** and **F**, Heat maps of
956 fragments per kilobase of transcript per million mapped reads (FPKM) values + 1 for all
957 significant DEGs from each treatment. Gene clusters are assigned based on second-
958 order and sub-clusters based on third- or fourth-order branching. Upregulated genes are
959 shown in yellow and downregulated genes in blue with intensity based on row z-score.
960 All DEGs in each plot for roots and shoots, respectively, are listed in **Supplemental Files**
961 **2 and 3**.

962

963 **Figure 4.** Expression patterns of genes encoding enzymes involved in the strigolactone
964 (**A**) and gibberellic acid (**B**) biosynthesis pathways in the roots of *Medicago truncatula*
965 colonized by arbuscular mycorrhizal fungi. Each diagram portrays the relative expression
966 levels of genes that encode components of the pathways shown as fragments per
967 kilobase of transcript per million mapped reads (FPKM; blue=low, yellow=high) in roots
968 from non-mycorrhizal (NM) plants or plants colonized by either *Glomus aggregatum* 165
969 (Ga165) or *Rhizophagus irregularis* 09 (Ri09). Letters within boxes indicate significant
970 differences (q-value < 0.05) in FPKM values between treatments and were determined
971 as part of the CuffDiff2 analysis (see **Supplemental Table S2**). Abbreviations: **A**, GAP,
972 glyceraldehyde 3-phosphate; DXS2, 1-deoxyxylulose 5-phosphate synthase2; MEP, 2-
973 methyl-erythritol-4-phosphate; GGDP geranylgeranyl pyrophosphate; D27, Dwarf27;
974 CCD, carotenoid cleavage dioxygenase; and PDR1a, pleiotropic drug resistance 1a. **B**,
975 CPS, *ent*-copalyl diphosphate synthase; KS, *ent*-kaurene synthase; KO, *ent*-kaurene
976 oxidase; KAO, *ent*-kaurenoic acid oxidase; GA13ox, gibberellin 13-oxidase; GA20ox,
977 gibberellin 20-oxidase; GA3ox, gibberellin 3-oxidase; and GA2ox, gibberellin 2-oxidase.

978

979 **Figure 5.** Relative expression of six genes in the roots of *Medicago truncatula* after
980 colonization with different arbuscular mycorrhizal fungi. Expression of **A**, *Required for*
981 *Arbuscule Development 1* (*RAD1*); **B**, *MYB-like Transcription Factor 1* (*MYB1*); **C**,
982 *Phosphate Transporter 8* (*PT8*); **D**, *Ammonium Transporter 2;3* (*AMT2;3*); **E**, *Reduced*
983 *Arbuscular Mycorrhization 2* (*RAM2*); and **F**, *Sugars Will Eventually Be Exported*
984 *Transporter 1.2* (*SWEET1.2*) in the roots of non-mycorrhizal plants (NM, n=3) and plants

985 inoculated with *Glomus aggregatum* 165 (Ga165, n=3) or *Rhizophagus irregularis* 09
986 (Ri09, n=4). Expression levels are shown as fragments per kilobase of transcript per
987 million mapped reads (FPKM). Data points represent individual values for biological
988 replicates (n = 5) and bars represent the mean of each treatment ± SEM. Significant
989 differences (q-value < 0.05) in FPKM values between treatments were determined as part
990 of the CuffDiff2 analysis and are indicated using different letters (see **Supplemental**
991 **Table S3**).
992
993 **Figure 6.** Expression patterns of significantly differentially expressed mineral transporter
994 genes in the roots of *Medicago truncatula* after colonization with different arbuscular
995 mycorrhizal fungi. **A**, Venn diagrams showing the number of mineral transporters that are
996 significantly up- (yellow) or down-regulated (blue) in roots colonized by *Glomus*
997 *aggregatum* 165 (Ga165) or *Rhizophagus irregularis* 09 (Ri09), or both. **B**, summary of
998 the number of genes from specific gene annotation groups of mineral transporters that
999 are up- or down-regulated in roots colonized by Ga165 or Ri09, or both (see also
1000 **Supplemental File 6**). Expression patterns of genes annotated as **C**, ammonium; **D**,
1001 nitrate; **E**, phosphate; and **F**, sulfate transporters in the roots of non-mycorrhizal plants
1002 (NM; n=3) and plants inoculated with Ga165 (n=3) or Ri09 (n=4). The bars in C–F
1003 represent the mean of each treatment ± SEM (data points for biological replicates are
1004 displayed in **Supplemental Figure S8**). Expression levels are shown as fragments per
1005 kilobase of transcript per million mapped reads (FPKM), only genes with FPKM ≥ 10 are
1006 shown, significant differences (q-value < 0.05) in FPKM values between treatments were

1007 determined as part of the CuffDiff2 analysis and are indicated using different letters on
1008 the bars.
1009
1010 **Figure 7.** Expression patterns of significantly differentially expressed secondary
1011 metabolite transporters in the roots of *Medicago truncatula* after colonization with different
1012 AM fungi. **A**, Venn diagrams showing the number of secondary metabolite transporters
1013 that are significantly up- (yellow) or down-regulated (blue) in roots colonized by *Glomus*
1014 *aggregatum* 165 (Ga165) or *Rhizophagus irregularis* 09 (Ri09), or both. **B**, summary of
1015 the number of genes from specific gene annotation groups of secondary metabolite
1016 transports that are up- or down-regulated in roots colonized by Ga165 or Ri09, or both
1017 (see **Supplemental File 7**). Expression patterns of genes annotated as **C**, ATP-binding
1018 cassette (ABC); **D**, amino acid or peptide; **E**, major facilitator superfamily (MFS) or major
1019 intrinsic protein (MIP); and **F**, SWEET transporters in the roots of non-mycorrhizal plants
1020 (NM; n = 3) and plants inoculated with Ga165 (n =3) or Ri09 (n = 4). The bars in C-F
1021 represent the mean of each treatment ± SEM (data points for biological replicates are
1022 displayed in **Supplemental Figure S9**). Expression levels are shown as fragments per
1023 kilobase of transcript per million mapped reads (FPKM); only genes with FPKM ≥ 10 are
1024 shown; significant differences (q-value < 0.05) in FPKM values between treatments were
1025 determined as part of the CuffDiff2 analysis and are indicated using different letters on
1026 the bars. Abbreviations in B: G3P, glycerol-3-phosphate; NAT, nucleobase-ascorbate
1027 transporter; OST, organic solute transporter; TPT, triose-phosphate transporter; TRAPP,
1028 transport protein particle.
1029

1030 **Figure 8.** Expression patterns of significantly differentially expressed genes in the shoots
1031 of *Medicago truncatula* colonized by different AM fungi. Expression levels of genes
1032 involved in **A**, photosynthesis; **B**, response to biotic stress; and **C**, response to abiotic
1033 stress in non-mycorrhizal plants (NM; n=4) or plants colonized by *Glomus aggregatum*
1034 165 (Ga165, n=4) or *Rhizophagus irregularis* 09 (Ri09, n=3). Bars represent the mean of
1035 each treatment ± SEM (data points for biological replicates are displayed in
1036 **Supplemental Figure S12**). Expression levels are shown as fragments per kilobase of
1037 transcript per million mapped reads (FPKM), and significant differences (q-value < 0.05)
1038 in FPKM values between treatments were determined as part of the CuffDiff2 analysis
1039 and are indicated using different letters above the bars (see also **Supplemental Table**
1040 **S4**).
1041
1042 **Figure 9.** Summary of the physiological and transcriptomic responses in roots and shoots
1043 of *Medicago truncatula* colonized by either *Glomus aggregatum* 165 or *Rhizophagus*
1044 *irregularis* 09. Physiological data include the analysis of AM colonization, plant biomass,
1045 and both phosphorus and nitrogen-15 contents in plant tissues. Transcriptomic data
1046 include the expression patterns of nutrient transporters and enrichment of gene ontology
1047 terms. Yellow up-arrows indicate an increase, equal signs (=) specify no change, and blue
1048 down-arrows designate a decrease in each response compared to non-mycorrhizal
1049 plants. Arrow size indicates the degree of the response.
1050
1051

1052 **SUPPORTING INFORMATION**

1053 **Supplemental Figure S1.** Schematic model of the dual-compartment pot system used
1054 for this study.

1055 **Supplemental Figure S2**. Shoot and root phosphorous concentration of *Medicago*
1056 *truncatula* colonized by arbuscular mycorrhizal fungi.

1057 **Supplemental Figure S3**. Hierarchical clustering of biological replicates from root RNA
1058 sequencing data.

1059 **Supplemental Figure S4**. Hierarchical clustering of biological replicates from shoot RNA
1060 sequencing data.

1061 **Supplemental Figure S5**. Volcano plots of differentially expressed genes (DEGs)
1062 between treatments.

1063 **Supplemental Figure S6**. Summary of gene ontology enrichment analysis of genes
1064 upregulated in the roots of *Medicago trunctaula*.

1065 **Supplemental Figure S7**. Summary of gene ontology enrichment analysis of genes
1066 downregulated in the roots of *Medicago trunctaula*.

1067 **Supplemental Figure S8**. Alternative portrayal of expression patterns of nutrient
1068 transporter genes.

1069 **Supplemental Figure S9**. Alternative portrayal of expression patterns of secondary
1070 metabolite transporter genes.

1071 **Supplemental Figure S10**. Summary of gene ontology enrichment analysis of
1072 differentially expressed genes in the shoots of *Medicago truncatula*.

1073 **Supplemental Figure S11**. Alternative portrayal of expression patterns of genes involved
1074 in photosynthesis, response to biotic stress, and response to abiotic stress.

1075 **Supplemental Table S1.** F statistics and p-values from one-way ANOVA for each
1076 experimental parameter.
1077 **Supplemental Table S2**. Expression levels of genes associated with the strigolactone
1078 biosynthesis pathway and the common symbiosis signaling pathway in roots of *Medicago*
1079 *truncatula*.
1080 **Supplemental Table S3**. Expression levels of genes downstream of the common
1081 symbiosis signaling pathway in roots of *Medicago truncatula*.
1082 **Supplemental Table S4**. List of differentially regulated genes from shoot gene ontology
1083 enrichment analysis.
1084 **Supplemental Table S5**. List of differentially regulated defense response genes from
1085 root gene ontology enrichment analysis.
1086 **Supplemental File 1**. Significantly differentially expressed genes in roots
1087 **Supplemental File 2**. Significantly differentially expressed genes in shoots
1088 **Supplemental File 3**. Significant gene ontology terms in roots
1089 **Supplemental File 4**. Significantly differentially expressed transporters in roots
1090 **Supplemental File 5**. List of mineral transporters by type
1091 **Supplemental File 6**. List of secondary metabolite transporters by type
1092 **Supplemental File 7**. Significant gene ontology terms in shoots
1093

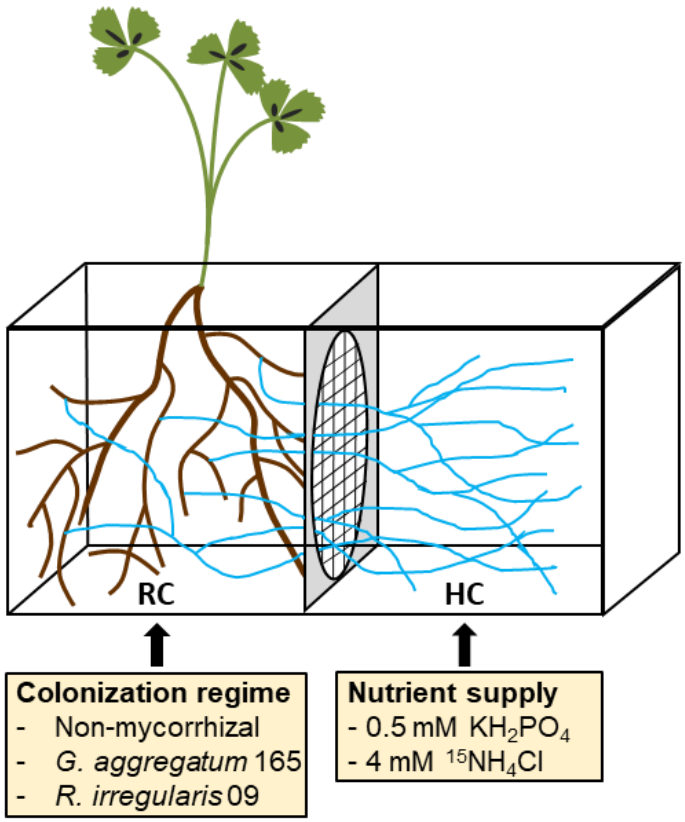

Supplemental Figure S1. Schematic model of the dual-compartment pot system used for this study. Roots in the root compartment (RC) were mock-inoculated for the non-mycorrhizal control treatment and for the mycorrhizal treatments, roots were inoculated with either 500 spores of either *Glomus aggregatum* 165 or *Rhizophagus irregularis* 09. Five weeks post-inoculation, 0.5 mM KH_2PO_4 and 4 mM $^{15}NH_4Cl$ were added to the hyphal compartment (HC).

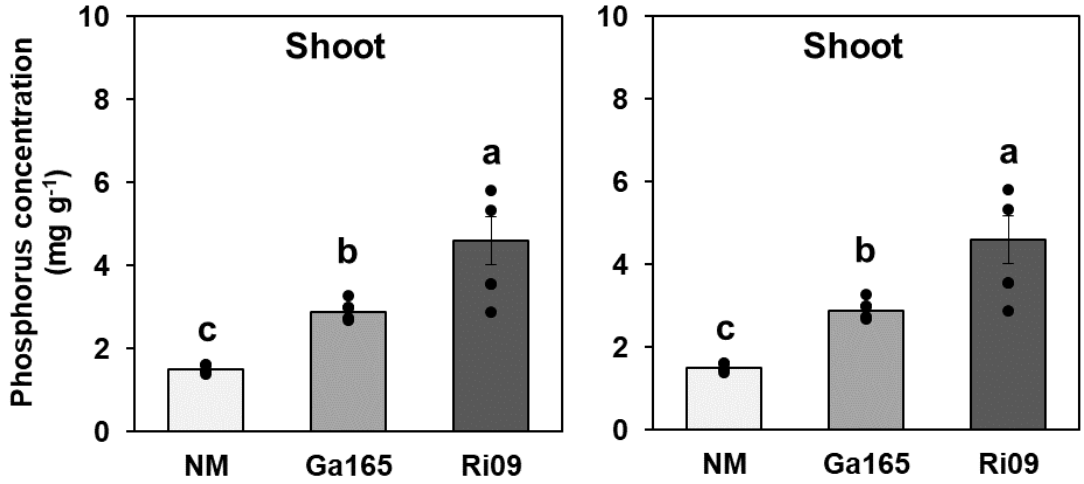

Supplemental Figure S2. Shoot and root phosphorous concentration of *Medicago truncatula* colonized by arbuscular mycorrhizal fungi. The plants were inoculated with either *Glomus aggregatum* 165 (Ga165) or *Rhizophagus irregularis* 09 (Ri09). Control plants were mock inoculated and served as non-mycorrhizal (NM) controls. Data points represent individual values for biological replicates (n = 5) and bars represent the mean of each treatment ± SEM. Different letters above the bars indicate statistically significant differences ($p \leq 0.05$) based on one-way ANOVA and LSD test. F statistics and p-values are shown in **Supplemental Table S1**.

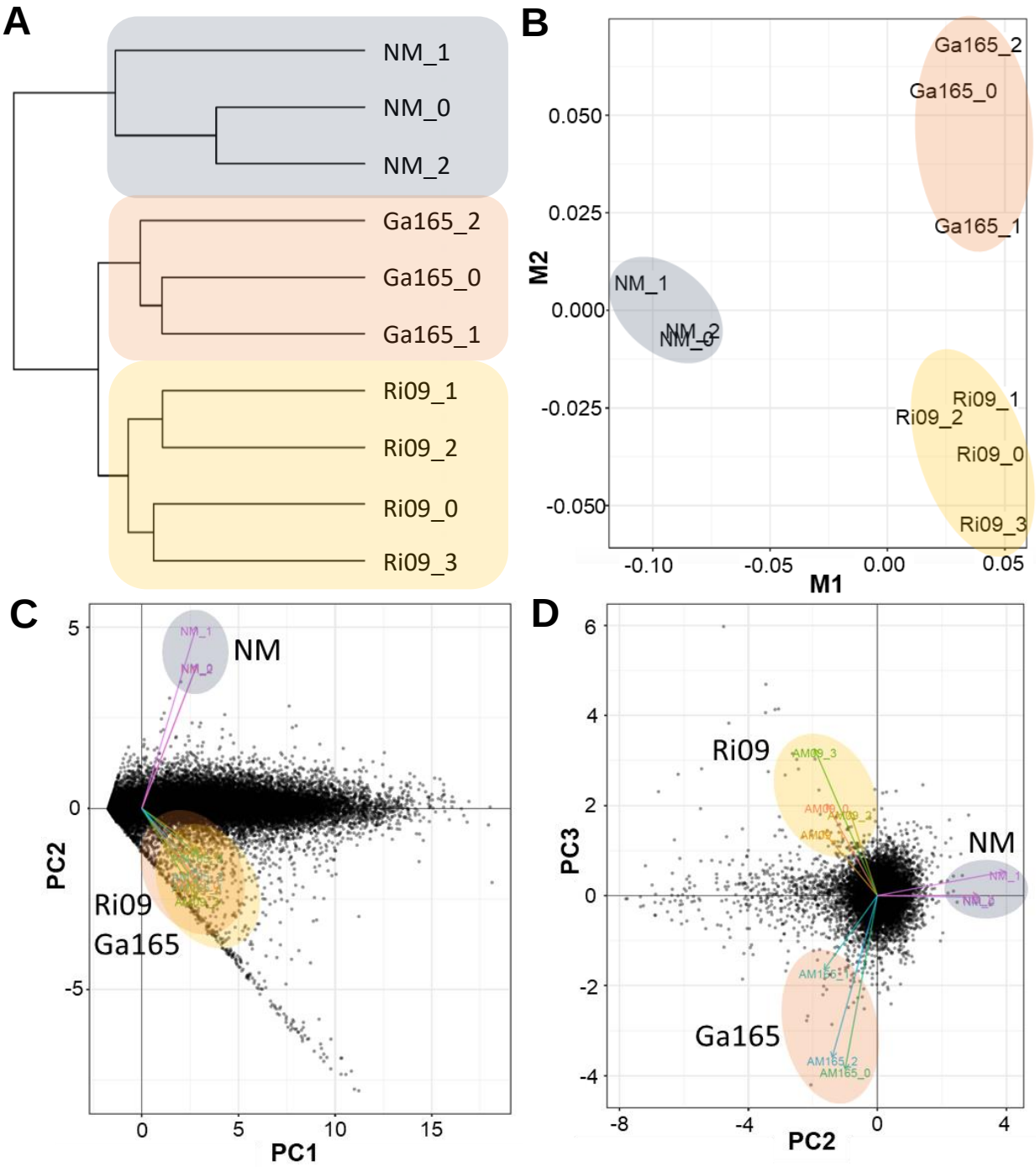

Supplemental Figure S3. Hierarchical clustering of biological replicates from root RNA sequencing data. Treatments include non-mycorrhizal (NM, n = 3), *Glomus aggregatum* 165 (Ga165, n = 3) and *Rhizophagus irregularis* 09 (Ri09, n = 4). The data were clustered using **A**, dendrogram analysis; **B**, multidimensional scaling; and principal component analyses (PCA), including PC1 vs. PC2 (**C**) and PC2 vs. PC3 (**D**). Note the distinct clustering of all biological replicates from each treatment.

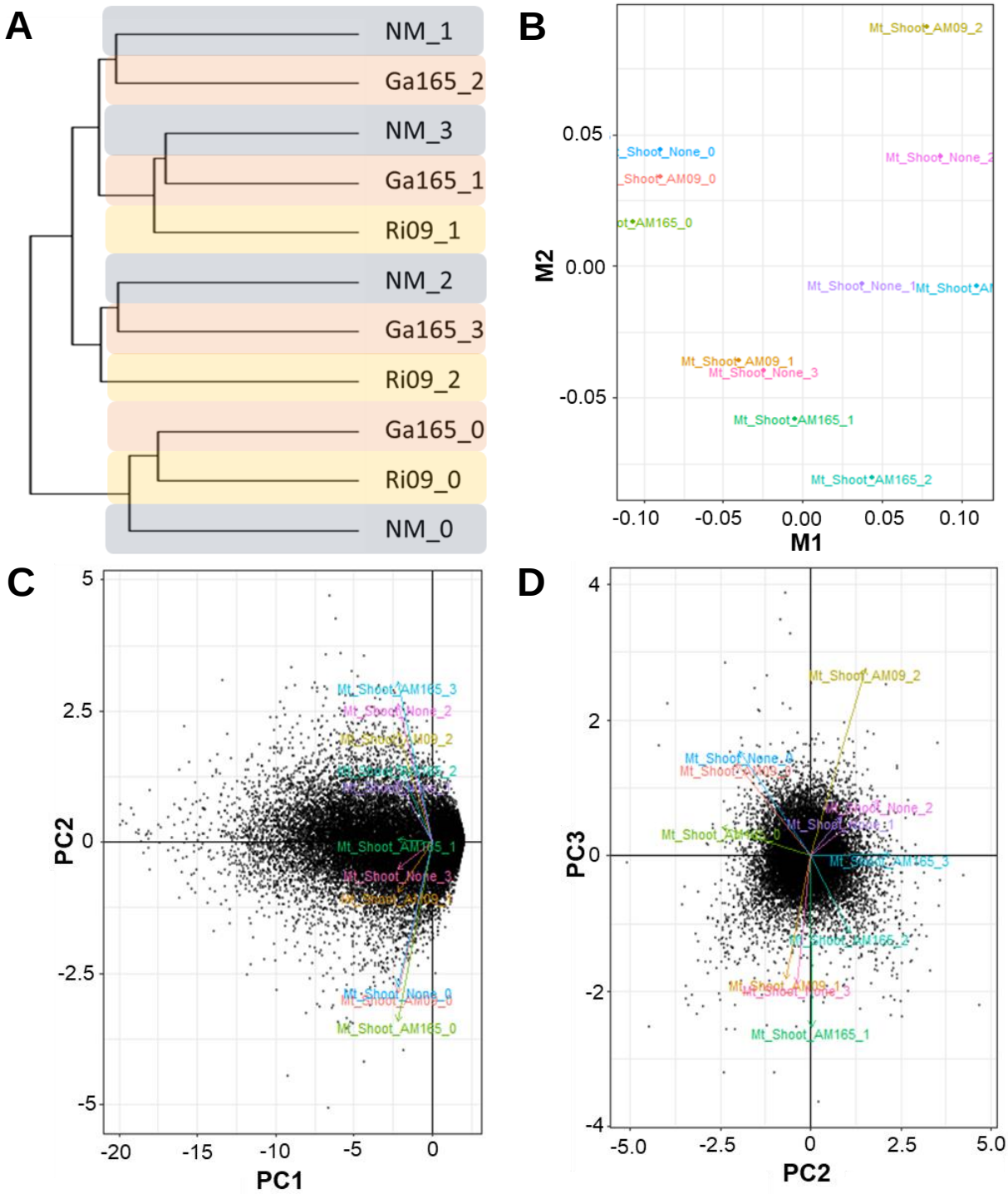

Supplemental Figure S4. Hierarchical clustering of biological replicates from shoot RNA sequencing data. Treatments include non-mycorrhizal (NM, n = 4), *Glomus aggregatum* 165 (Ga165, n = 4) and *Rhizophagus irregularis* 09 (Ri09, n = 3). The data were clustered using **A**, dendrogram analysis; **B**, multidimensional scaling; and **C-D**, principal component analyses (PCA), including PC1 vs. PC2 (**C**) and PC2 vs. PC3 (**D**). Note that no distinct clustering of biological replicates was observed for any of the treatments.

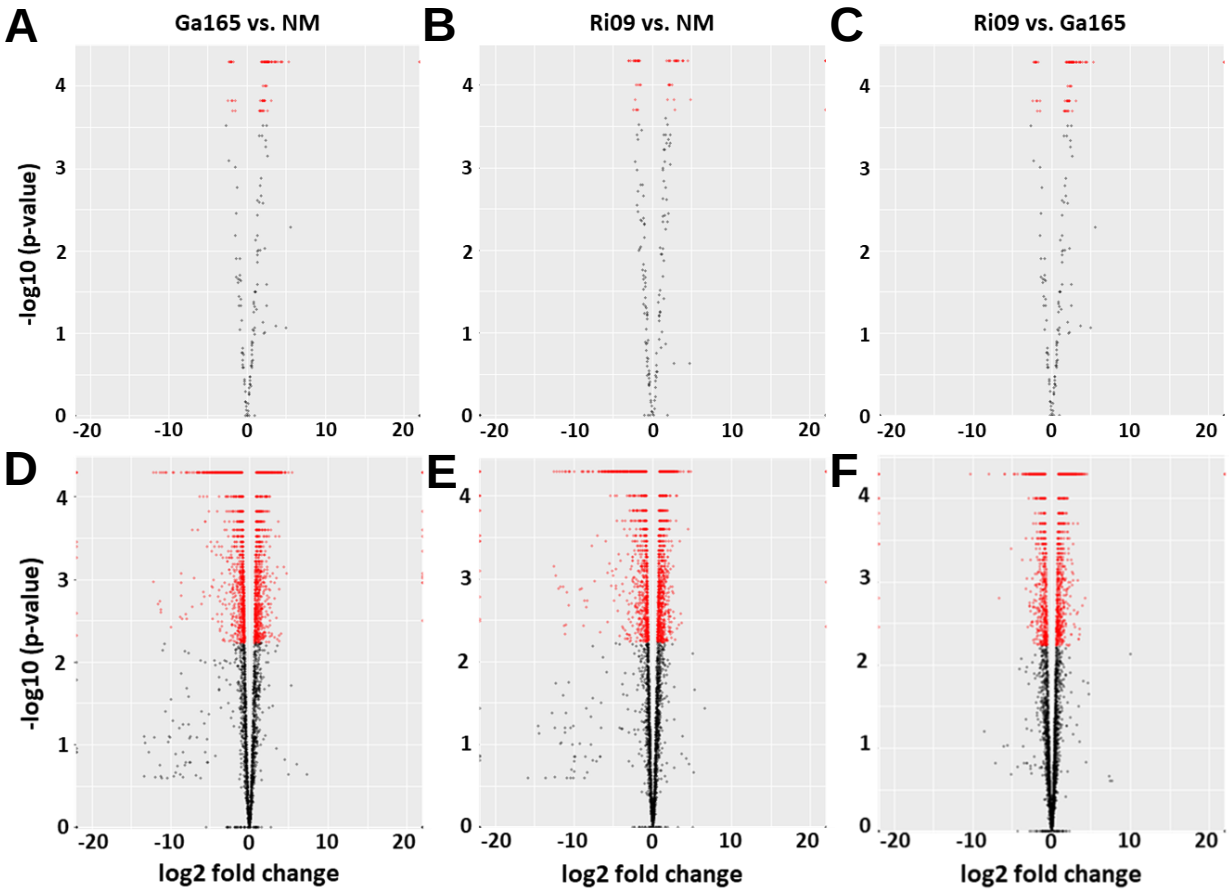

Supplemental Figure S5. Volcano plots of differentially expressed genes (DEGs) between treatments. **A-C**, shoot data are shown on top and **D-F**, root data on bottom for the following comparisons: left, *Glomus aggregatum* 165 (Ga165) vs. non-mycorrhizal (NM); middle, *Rhizophagus irregularis* 09 (Ri09) vs. NM; and right, Ri09 vs. Ga165. Data points representing significant DEGs ($-\log_{10}$[p-value] > 2.3) are shown in red while non-significant DEGs ($-\log_{10}$[p-value] < 2.3) are shown in black. Note the greater abundance of significant DEGs among the root data compared to the shoot data.

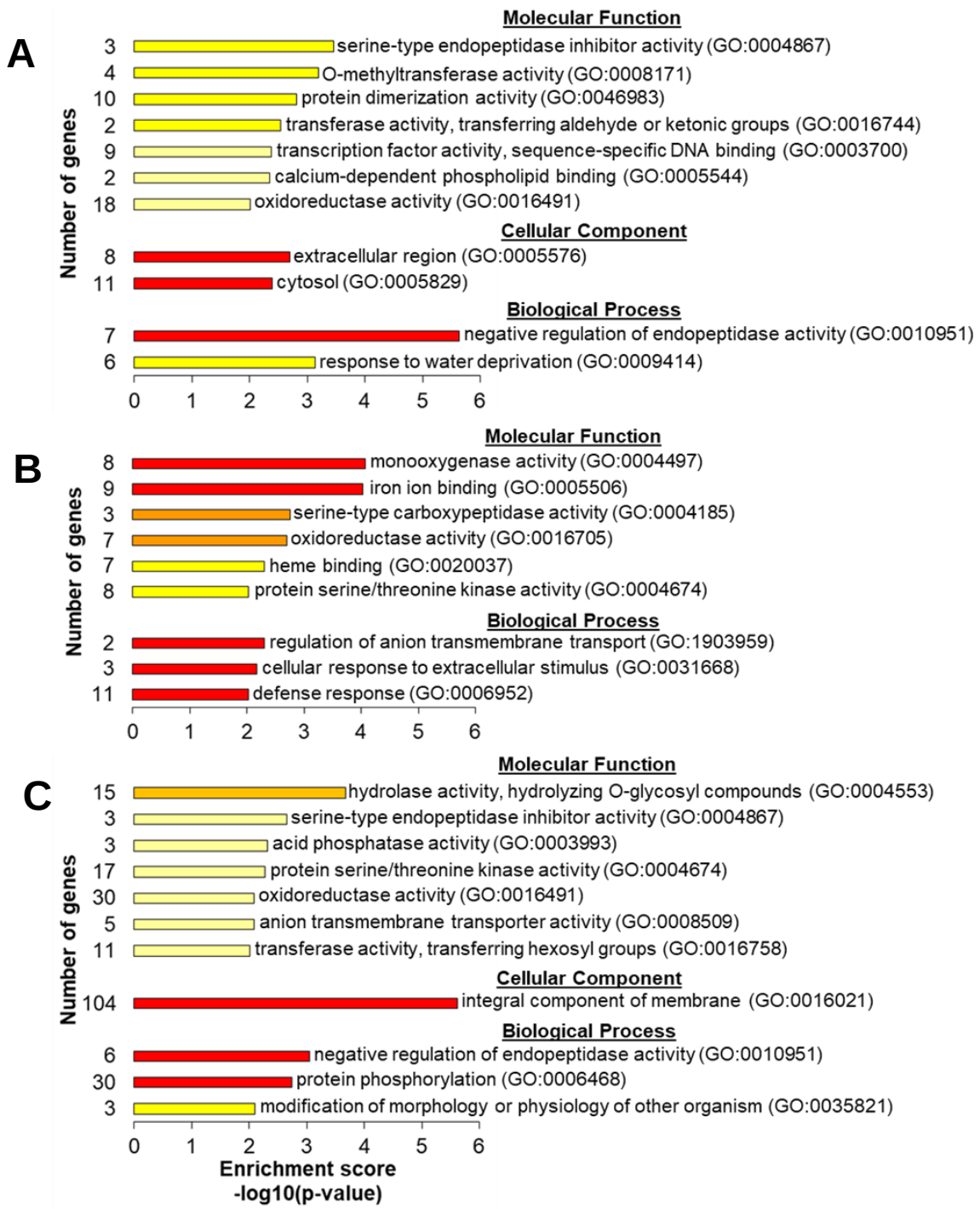

Supplemental Figure S6. Summary of gene ontology enrichment analysis of genes upregulated in the roots of *Medicago truncatula*. All enriched gene ontology (GO) terms for **A**, *Glomus aggregatum* 165; **B**, *Rhizophagus irregularis* 09; or **C**, both species are shown for molecular function, cellular component, and biological process. The enrichment score ($-\log_{10}$[p-value]) for each GO term is also shown ranging from low (light yellow) to high (red). A list of the genes from each GO term can be found in **Supplemental File 4**.

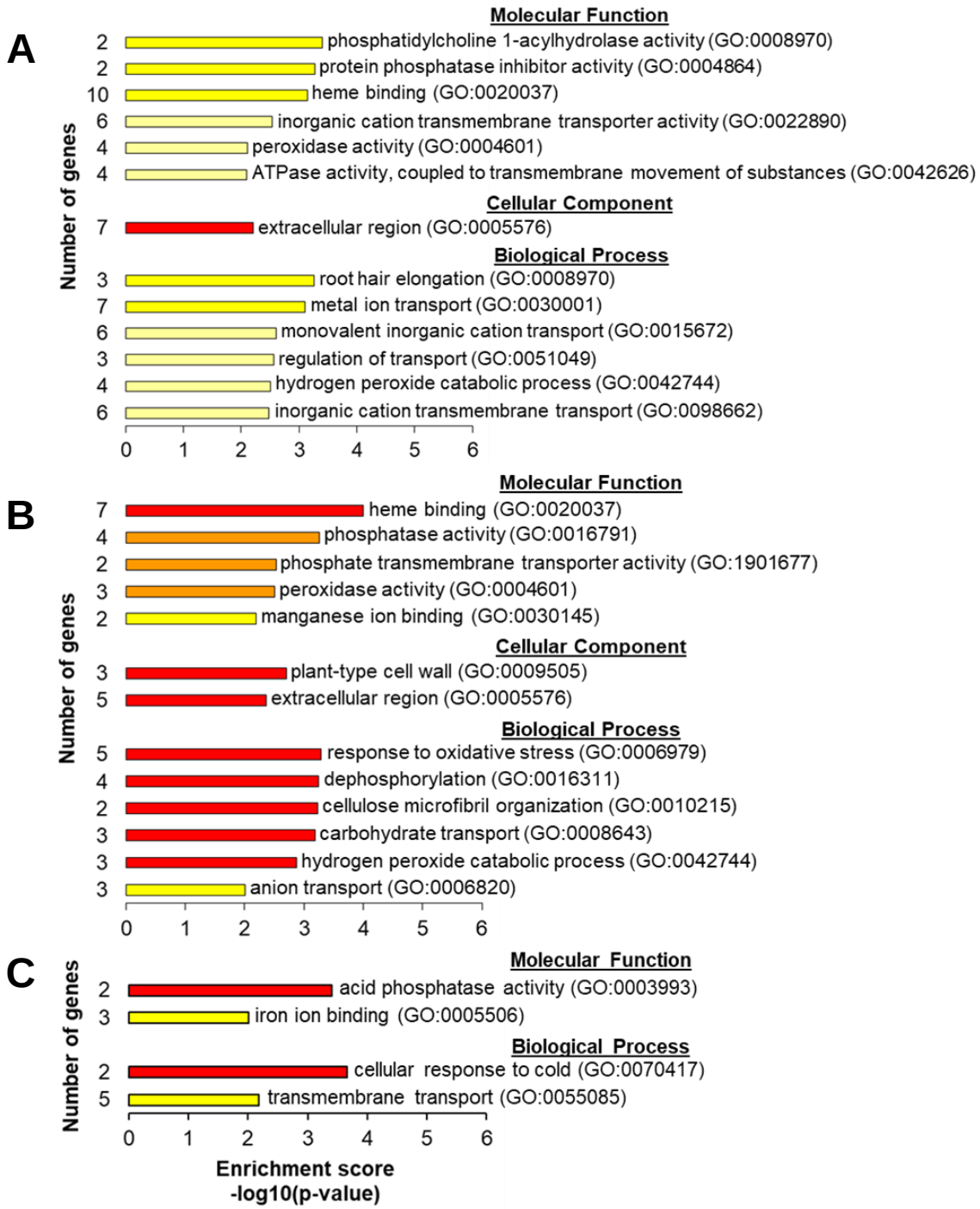

Supplemental Figure S7. Summary of gene ontology enrichment analysis of genes downregulated in the roots of *Medicago trunctaula*. All enriched gene ontology (GO) terms for **A**, *Glomus aggregatum* 165; **B**, *Rhizophagus irregularis* 09; or **C**, both species are shown for molecular function, cellular component, and biological process. The enrichment score ($-\log_{10}$[p-value]) for each GO term is also shown ranging from low (light yellow) to high (red). A list of the genes from each GO term can be found in **Supplemental File 4**.

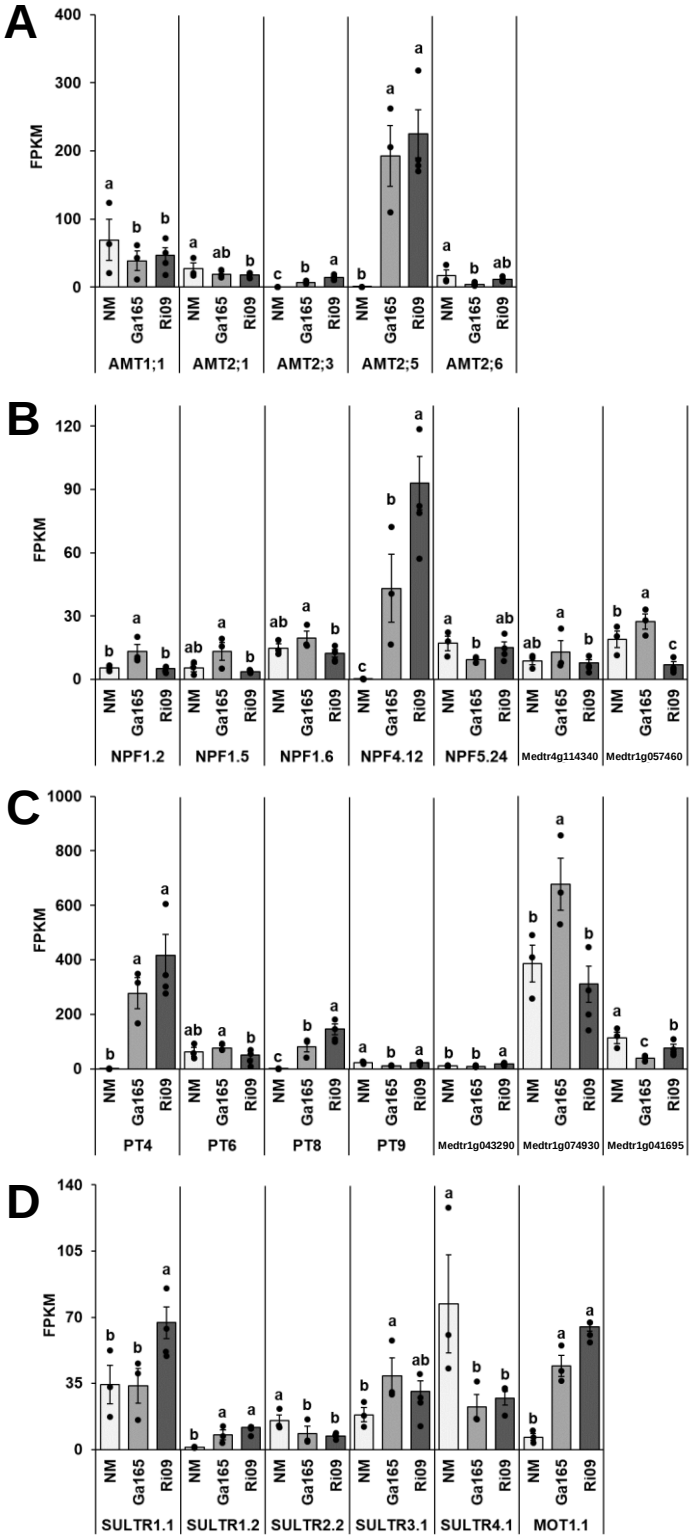

Supplemental Figure S8. Alternative portrayal of expression patterns of genes annotated as **A**, ammonium; **B**, nitrate; **C**, phosphate; and **D**, sulfate transporters. Shown are individual data points for gene expression values from each biological replicate overlayed on the graphs from **Figure 6**, panels C through F, respectively.

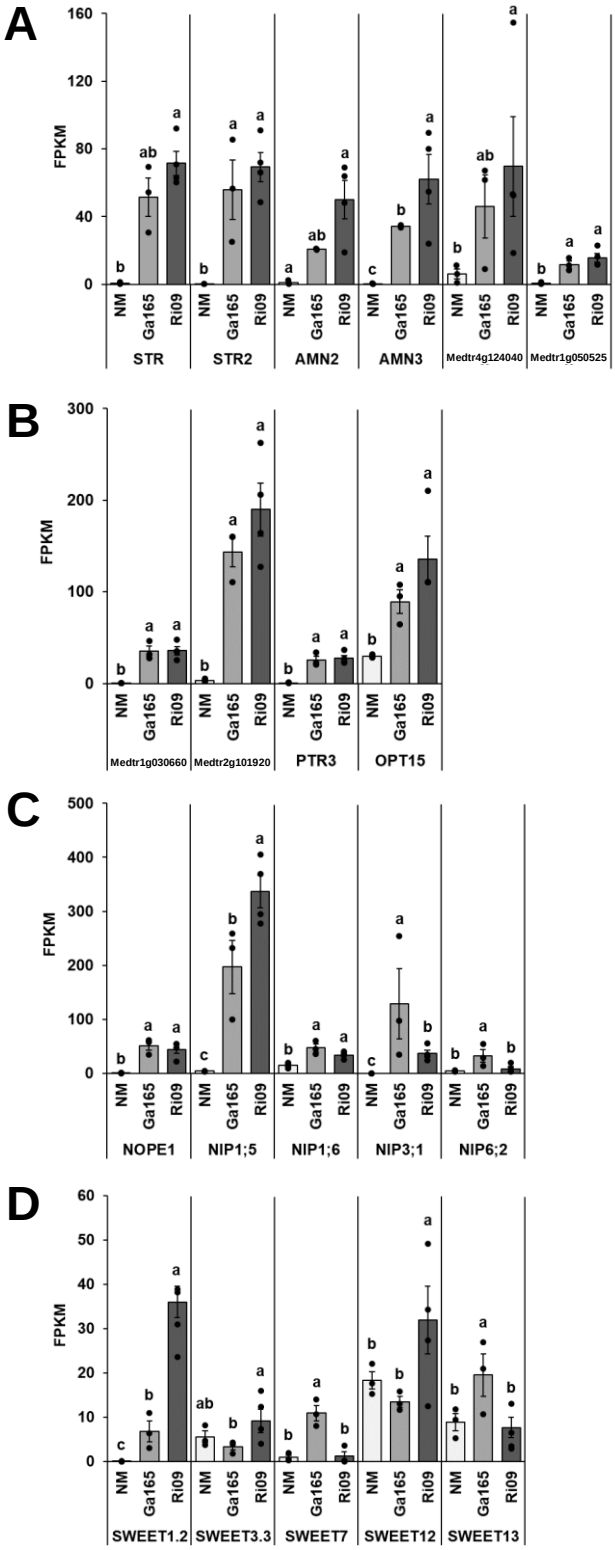

Supplemental Figure S9. Alternative portrayal of expression patterns of genes annotated as **A**, ABC; **B**, amino acid or peptide; **C**, MIP or MFS; and **D**, SWEET transporters. Shown are individual data points for gene expression values from each biological replicate overlayed on the graphs from **Figure 7**, panels C through F, respectively.

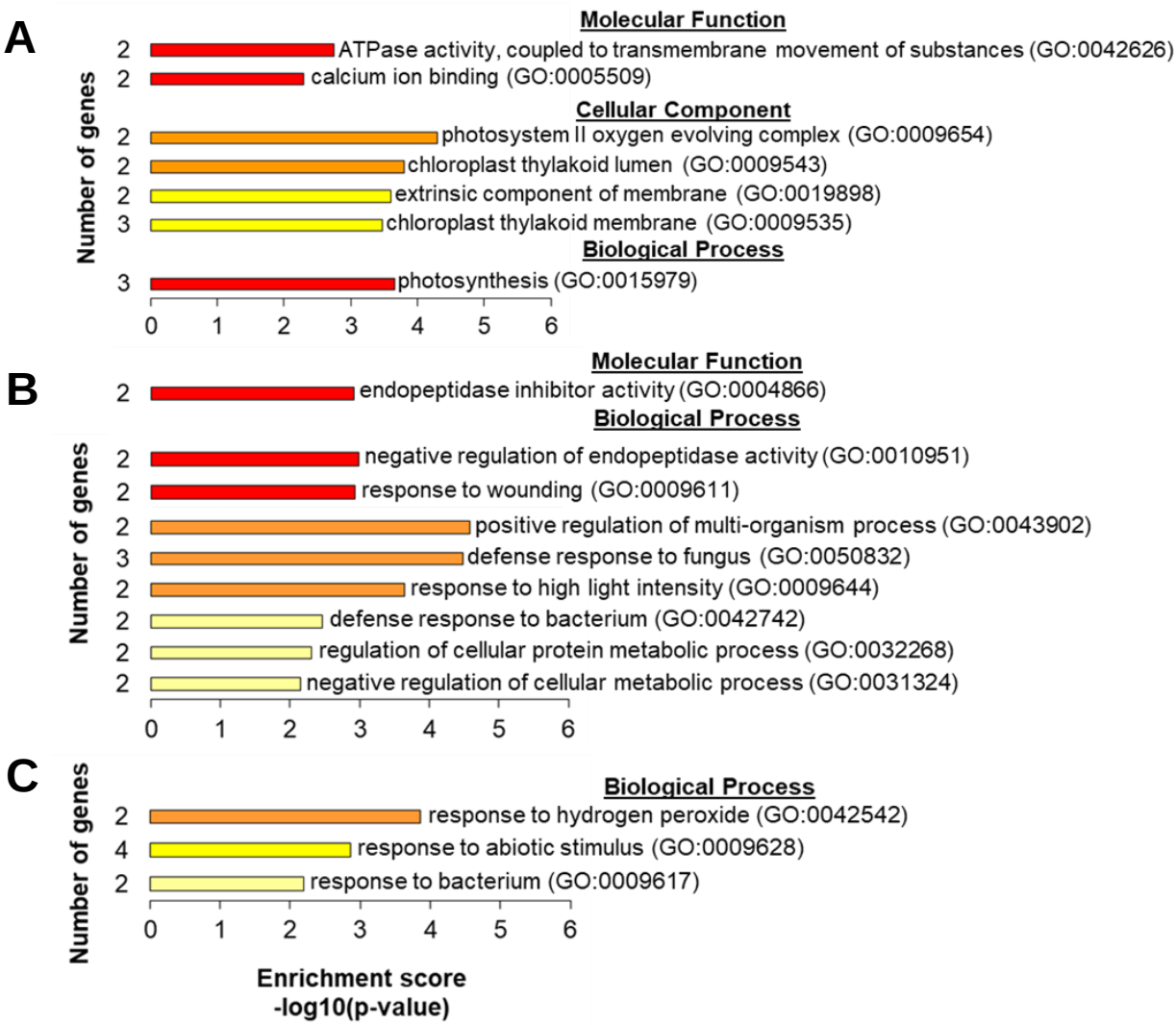

Supplemental Figure S10. Summary of gene ontology enrichment analysis of differentially expressed genes in the shoots of *Medicago trunctaula*. Enriched gene ontology (GO) terms for molecular function, cellular component, and biological process among the following groups of genes based on the heatmap in **Figure 2F**: **A**, genes upregulated in the shoots of plants colonized by *Rhizophagus irregularis* 09 (Ri09); **B**, genes upregulated in the shoots of plants colonized by *Glomus aggregatum* 165 (Ga165); and **C**, genes downregulated in the shoots of plants colonized by Ri09. The enrichment score ($-\log_{10}$[p-value]) for each GO term is also shown ranging from low (light yellow) to high (red). A list of the genes from each GO term can be found in **Supplemental File 8**.

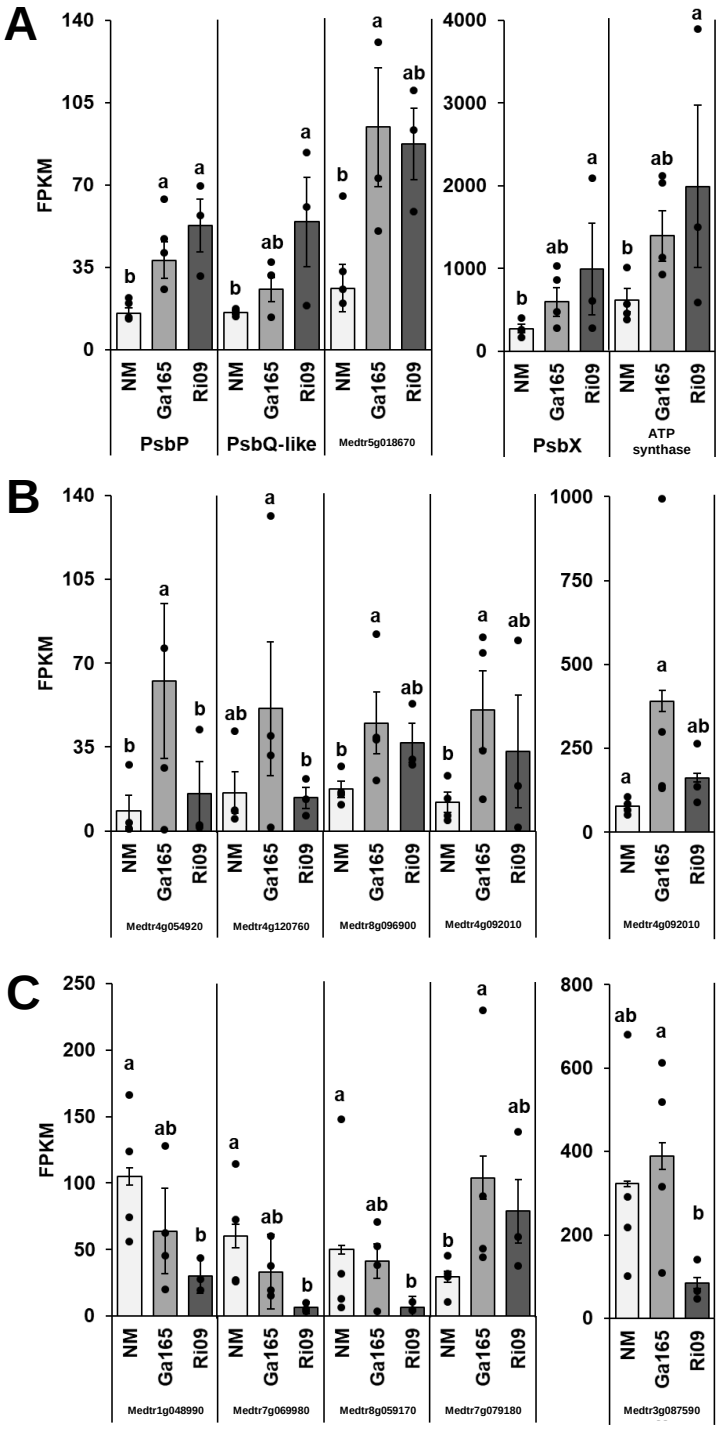

Supplemental Figure S11. Alternative portrayal of expression patterns of genes involved in **A**, photosynthesis; **B**, response to biotic stress; and **C**, response to abiotic stress. Shown are individual data points for gene expression values from each biological replicate overlayed on the graphs from **Figure 8**, panels A through B, respectively.

Supplemental Table S1. F statistics and p-values from one-way ANOVA for each experimental parameter.

Parameter	F statistics	p-value
Shoot dry wt. (g)	$F_{2,14} = 16.61$	0.0003
Root dry wt. (g)	$F_{2,14} = 13.14$	0.0009
Shoot P concentration (mg/g)	$F_{2,14} = 21.17$	<0.0001
Total shoot P content (mg)	$F_{2,14} = 26.79$	<0.0001
Root P concentration (mg/g)	$F_{2,14} = 127.01$	<0.0001
Total root P content (mg)	$F_{2,14} = 136.80$	<0.0001
Shoot ^{15}N enrichment (%)	$F_{2,14} = 12.01$	0.0014
Root ^{15}N enrichment (%)	$F_{2,14} = 49.75$	<0.0001

Supplemental Table S2. Expression levels of genes associated with the strigolactone biosynthesis pathway, the common symbiosis signaling pathway, and the gibberellic biosynthesis and degradation pathway in roots of *Medicago truncatula*. Mean FPKM (Fragments Per Kilobase of transcript per Million mapped reads) values for all listed genes are shown for all three treatments from this study, including nonmycorrhizal (NM, n=3) control plants and both *Glomus aggregatum* 165 (Ga165, n=3) and *Rhizophagus irregularis* 09 (Ri09, n=4) mycorrhizal plants. A green (low) to red (high) color scale is used to highlight differences in FPKM values. Significant differences (q-value < 0.05) in FPKM values between treatments were determined as part of the CuffDiff2 analysis and are indicated using different letters. References for the studies in which each gene was characterized are also included. Full citations can be found in the **Supplemental References**.

	Gene ID	Gene Name	NM		Ga165		Ri09		Reference
Strigolactone Biosynthesis & Transport	*Medtr8g068265*	*DXS2*	9.37	b	37.77	a	36.07	a	(Floß et al., 2008)
	Medtr1g471050	*D27*	37.83	b	64.74	a	80.61	a	(Müller et al., 2019)
	Medtr7g045370	*CCD7*	21.91	ab	15.87	b	28.47	a	(Gomez-Roldan et al., 2008)
	Medtr3g109610	*CCD8-1*	49.43	a	47.47	a	65.00	a	(Gomez-Roldan et al., 2008)
	Medtr3g104560	*MAX1a*	82.93	b	70.28	b	140.84	a	(Müller et al., 2019)
	Medtr8g020840	*NSP1*	6.02	c	13.98	b	22.41	a	(Liu et al., 2011)
	Medtr3g072710	*NSP2*	13.47	b	12.39	b	23.85	a	(Liu et al., 2011)
	Medtr3g107870	*PDR1a*	0.34	a	3.19	a	1.26	a	(Kretzschmar et al., 2012)
Common Symbiosis Signaling Pathway	*Medtr5g019040*	*NFP*	2.63	a	0.79	b	0.99	b	(Feng et al., 2019)
	Medtr3g080050	*LYK9*	0.88	a	2.37	a	0.27	a	(Gibelin-Viala et al., 2019)
	Medtr5g030920	*DMI2/NORK*	61.59	a	59.99	a	68.39	a	(Stracke et al., 2002)
	Medtr5g083030	*PUB1*	8.48	b	14.21	a	17.74	a	(Vernié et al., 2016)
	Medtr5g026500	*HMGR1*	29.53	a	35.08	a	22.69	a	(Kevei et al., 2007)
	Medtr2g005870	*DMI1*	3.42	a	2.91	a	3.95	a	(Ané et al., 2004)
	Medtr7g117580	*CASTOR*	20.94	a	25.02	a	26.92	a	(Charpentier et al., 2008)
	Medtr7g100110	*MCA8*	53.22	a	66.33	a	71.46	a	(Capoen et al., 2011)
	Medtr1g064240	*CNGC15a*	0.00	a	0.00	a	0.01	a	(Charpentier et al., 2016)
	Medtr4g058730	*CNGC15b*	0.29	a	3.98	a	6.61	a	(Charpentier et al., 2016)
	Medtr2g094860	*CNGC15c*	0.67	a	0.05	a	0.29	a	(Charpentier et al., 2016)
	Medtr8g043970	*DMI3/CCaMK*	19.29	a	19.19	a	16.05	a	(Lévy et al., 2004)
	Medtr5g026850	*IPD3/CYCLOPS*	25.28	a	33.95	a	37.35	a	(Horváth et al., 2011)
	Medtr3g065980	*DELLA1*	65.07	a	38.27	a	56.47	a	(Floss et al., 2013)
	Medtr4g122240	*DELLA2*	2.91	a	3.56	a	3.04	a	(Floss et al., 2013)
Gibberellic Acid	Medtr7g011663	CPS	17.09	a	11.06	ab	9.34	b	(Igielski et al., 2017)
	Medtr2g064295	KS	6.62	a	5.17	a	4.07	a	(Igielski et al., 2017)
	Medtr2g105360	KO	43.47	b	50.49	b	76.47	a	(Igielski et al., 2017)
	Medtr2g031930	KAO1	30.06	a	29.73	a	26.21	a	(Igielski et al., 2017)
	Medtr3g093530	CYP714_A1/GA13ox	6.71	b	13.26	a	10.26	ab	(Igielski et al., 2017)
	Medtr1g102070	GA20ox1	5.36	b	12.48	a	8.23	ab	(Igielski et al., 2017)
	Medtr1g086550	GA20ox6	7.66	c	41.71	a	16.02	b	(Nouri et al., 2021)
	Medtr8g033380	GA20ox8	0.16	c	8.21	a	2.42	b	(Igielski et al., 2017)
	Medtr2g102570	GA3ox1	10.68	a	7.96	ab	5.24	b	(Igielski et al., 2017)
	Medtr2g019370	GA2ox1	0.96	c	16.73	a	9.99	b	(Nouri et al., 2021)

Supplemental Table S3. Expression levels of genes downstream of the common symbiosis signaling pathway in roots of *Medicago truncatula*. Mean FPKM (Fragments Per Kilobase of transcript per Million mapped reads) values for all listed genes are shown for all three treatments from this study, including nonmycorrhizal (NM, n=3) control plants and both *Glomus aggregatum* 165 (Ga165, n=3) and *Rhizophagus irregularis* 09 (Ri09, n=4) mycorrhizal plants. A green (low) to red (high) color scale is used to highlight differences in FPKM values. Significant differences (q-value < 0.05) in FPKM values between treatments were determined as part of the CuffDiff2 analysis and are indicated using different letters. References for the studies in which each gene was identified as playing a role in the arbuscular mycorrhizal symbiosis are also included. Full citations can be found in the **Supplemental References**.

	Gene ID	Gene Name	NM		Ga165		Ri09		Reference
Transcription Factors	*Medtr7g027190*	*RAM1*	0.01	b	45.05	a	52.08	a	(Park et al., 2015)
	Medtr4g104020	*RAD1*	0.09	c	84.69	b	139.93	a	(Park et al., 2015)
	Medtr7g088990	*DIP1*	111.61	a	145.81	a	137.94	a	(Yu et al., 2014)
	Medtr2g034280	*MIG1*	0.56	a	0.97	a	1.15	a	(Heck et al., 2016)
	Medtr2g034260	*MIG2*	9.07	b	20.31	a	18.69	a	(Heck et al., 2016)
	Medtr2g034250	*MIG3*	7.73	b	18.70	a	25.75	a	(Heck et al., 2016)
	Medtr7g068600	*MYB1*	0.06	c	594.35	b	1262.52	a	(Floss et al., 2017)
Cellular Remodeling	*Medtr6g027840*	*VAPYRIN/VPY*	3.20	b	34.54	a	33.33	a	(Pumplin et al., 2010)
	Medtr1g017910	*EXO70I*	2.53	b	24.18	a	18.44	a	(Zhang et al., 2015)
	Medtr2g088700	*SYP132A*	56.60	b	92.13	a	79.90	ab	(Pan et al., 2016)
Lipid Biosynthesis & Transport	*Medtr8g468920*	*WRI5a*	0.00	b	2.26	a	3.15	a	(Jiang et al., 2018)
	Medtr8g107450	*STR*	0.68	b	51.53	b	71.44	a	(Zhang et al., 2010)
	Medtr5g030910	*STR2*	0.22	b	55.77	a	69.28	a	(Zhang et al., 2010)
	Medtr1g040500	*RAM2*	0.23	c	192.67	b	353.74	a	(Luginbuehl et al., 2017)
	Medtr1g109110	*FatM*	0.07	a	12.57	a	17.47	a	(Bravo et al., 2017)
Mineral Transport	*Medtr1g028600*	*PT4*	0.09	b	277.24	a	381.65	a	(Javot et al., 2007)
	Medtr5g068140	*PT8*	0.05	c	81.31	b	133.25	a	(Breuillin-Sessoms et al., 2015)
	Medtr8g074750	*AMT2;3*	0.00	c	7.08	b	13.07	a	(Breuillin-Sessoms et al., 2015)
	Medtr7g115050	*AMT2;4*	0.15	b	6.53	a	3.59	a	(Breuillin-Sessoms et al., 2015)
	Medtr1g036410	*AMT2;5*	0.11	b	192.75	a	213.55	a	(Breuillin-Sessoms et al., 2015)
Sugar Transport	*Medtr3g089125*	*SWEET1.2*	0.04	c	6.81	b	32.93	a	(An et al., 2019)

Supplemental Table S4. List of differentially regulated genes from shoot gene ontology enrichment analysis. Mean FPKM (Fragments Per Kilobase of transcript per Million mapped reads) values for all listed genes are shown for all three treatments from this study, including nonmycorrhizal (NM, n=3) control plants and both *Glomus aggregatum* 165 (Ga165, n=3) and *Rhizophagus irregularis* 09 (Ri09, n=4) mycorrhizal plants. A green (low) to red (high) color scale is used to highlight differences in FPKM values. Significant differences (q-value < 0.05) in FPKM values between treatments were determined as part of the CuffDiff2 analysis and are indicated using different letters.

	Gene ID	Gene Annotation	NM		Ga165		Ri09	
Photosynthesis	*Medtr1g015290*	ultraviolet-B-repressible protein	268.2	b	662.9	ab	992.1	a
	Medtr2g082580	oxygen-evolving enhancer protein	15.9	b	28.6	ab	54.4	a
	Medtr1g115410	photosystem II reaction center PsbP family protein	17.3	b	44.6	a	52.8	a
	Medtr1588s0010	ATP synthase F1, gamma subunit	605.3	b	1556.0	ab	1993.1	a
	Medtr6g084320	ABC transporter-like family-protein	12.8	b	21.8	ab	47.0	a
Biotic Stress	*Medtr4g054920*	cytochrome P450 family 94 protein	8.26	b	62.56	a	15.45	b
	Medtr4g120760	pathogenesis-related protein bet V I family protein	16.02	ab	51.03	a	13.83	b
	Medtr5g053950	allene oxide cyclase	77.55	b	391.10	a	162.61	ab
	Medtr8g096900	pathogenesis-related thaumatin family protein	17.47	b	45.09	a	36.91	ab
	Medtr4g092010	(3S)-linalool/(E)-nerolidol/(E,E)-geranyl linalool synthase	11.90	b	50.43	a	33.24	ab
Abiotic Stress	*Medtr1g048990*	superoxide dismutase	105.08	a	63.93	ab	30.32	b
	Medtr3g087590	myo-inositol 1-phosphate synthase	322.70	ab	388.70	a	84.82	b
	Medtr7g069980	ferritin	60.16	a	33.23	a	6.36	b
	Medtr8g059170	NAC transcription factor-like protein	49.87	a	41.35	a	6.64	b
	Medtr5g018670	photosystem II oxygen-evolving enhancer protein	35.97	b	103.56	a	87.44	ab
	Medtr7g079180	late embryogenesis abundant protein	29.47	b	103.91	a	78.75	ab

Supplemental Table S5. List of differentially regulated defense response genes from root gene ontology enrichment analysis. Mean FPKM (Fragments Per Kilobase of transcript per Million mapped reads) values for all listed genes are shown for all three treatments from this study, including nonmycorrhizal (NM, n=3) control plants and both *Glomus aggregatum* 165 (Ga165, n=3) and *Rhizophagus irregularis* 09 (Ri09, n=4) mycorrhizal plants. A green (low) to red (high) color scale is used to highlight differences in FPKM values. Significant differences (q-value < 0.05) in FPKM values between treatments were determined as part of the CuffDiff2 analysis and are indicated using different letters.

	Gene ID	Gene Annotation	NM		Ga165		Ri09	
Defense Response	*Medtr0012s0290*	disease resistance protein (TIR-NBS-LRR class), putative	0.91	a	3.53	b	5.78	c
	Medtr1g015140	WRKY family transcription factor	0.67	a	1.06	ab	2.68	b
	Medtr2g008430	LL-diaminopimelate aminotransferase	2.08	a	7.54	b	14.17	c
	Medtr3g028040	LRR and NB-ARC domain disease resistance protein	0.08	a	0.53	ab	1.10	b
	Medtr3g072140	disease resistance protein (TIR-NBS-LRR class), putative	0.15	a	0.56	ab	0.82	b
	Medtr6g006990	carbonic anhydrase family protein	0.56	a	3.53	ab	7.55	b
	Medtr8g012810	Defensin related	0.00	a	0.67	ab	45.59	b
	Medtr8g012815	Defensin related	0.00	a	1.00	ab	34.68	b
	Medtr8g012845	Defensin related	0.00	a	0.36	ab	51.54	b
	Medtr8g012870	Defensin related	0.00	a	0.49	ab	5.59	b
	Medtr8g059405	Defensin	0.97	a	0.73	a	8.89	b